UNIVERSITÀ
DEGLI STUDI
DI PADOVA

DIPARTIMENTO
DI INGEGNERIA
DELL'INFORMAZIONE

DIPARTIMENTO DI INGEGNERIA DELL'INFORMAZIONE

CORSO DI LAUREA IN INGEGNERIA DELL'INFORMAZIONE

LASER-DRIVEN LIGHT SAILS, A POSSIBLE WAY FOR INTERSTELLAR EXPLORATION

Relatore: Prof. / Dott.sa MARIA GUGLIELMINA PELIZZO

Laureando: TRENTI STEFANO

ANNO ACCADEMICO 2021 – 2022

19 Luglio 2022

Contents

1 Introduction **1**

2 Means of Laser Propulsion **3**

2.1 Laser Electric Propulsion 3

2.2 Laser Thermal Propulsion 4

2.3 Laser Sails 6

2.4 Sail-type designs 7

2.5 Laser Launch System 8

2.6 Current projects 10

3 Laser Propulsion by radiation pressure: theory of the sail **11**

3.1 Classical model derivation 11

3.2 Relativistic model derivation 13

4 Sail's material characteristics **19**

5 Coasting and Deceleration phases **27**

5.1 Coasting phase 27

5.2 Deceleration phase 31

6 Conclusions **35**

1 Introduction

The human species has made tremendous advances in space exploration in the last century, from being able to launch the first satellite Sputnik in 1957 to sending autonomous rovers on the surface on Mars. As we pursue the exploration of outer space a new question arises, what lies ahead? What is the next possible step to follow after examining our own solar system? The next objective must lie beyond the limits of our planetary system, interstellar exploration and the search for life outside of Earth. This will be the toughest challenge faced yet as, once you exit the solar system, the scale of things becomes so vast as much as to make them difficult to comprehend. So far the object that humans managed to send the furthest into space is Voyager 1. This space probe was launched by NASA in 1977 and as of July 2022 it has travelled more than 23 billion kilometres, or about 156 Astronomical Units. This is an enormous distance, however by considering the space between star systems in the universe this remoteness is put into perspective. For example the closest star system to our planet is the Alpha Centauri system, which is around 41 trillion kilometres away from earth or about 274068 AU. The total distance traveled by Voyager in 44 years is just a small fraction (about 0.05%) of the total trip length from Earth to Alpha Centauri. It would take Voyager 1 another 78,390 years to travel the remaining distance. This is an absurd long time-frame, about 934 generations of human beings would pass before the completion of this trip. The ultimate goal would be to accomplish this journey in a trip-time smaller than a human lifetime.

Figure 1: Artistic interpretation of a Light-Sail arriving on Proxima b.[1]

[1]Credit: L. Calçada/ESO

To achieve this, a completely new paradigm for interstellar space travel must be conceived. Traditional probe designs will never be able to achieve interstellar travel in that time frame. The chosen destination for the first Interstellar trip is the Alpha Centauri system. Not only this is the nearest star system to Earth, it also has three confirmed exo-planets and more candidates detected but yet to be confirmed. A main candidate for exploration is a planet orbiting Proxima Centauri, one of the stars of this triple star system. This planet called Proxima b is found in the habitable zone, meaning that it could be a candidate to host alien life. To accomplish this journey in the desired time-frame then a terminal velocity of 25% the speed of light is chosen as an ultimate target, which could make the trip-time smaller than 25 years. The journey of this probe would consist of three main phases: the acceleration phase, the coasting phase and the deceleration phase. The first step to explore this system would have to be to send a small un-crewed fly-by exploration mission. There are plenty different ideas on how to achieve this goal, some more fictional than others. Exotic propulsion methods can be divided in sub-light speed and faster-than-light speed concepts. Faster-than-light travel ideas are highly speculative concepts that exploit edge cases of known physics and have no proven feasibility. This makes them unsuitable for interstellar exploration in the next few decades. An example of these latter concepts is the Alcubierre warp drive, this idea use exotic matter with negative mass to contract space-time in front of the vehicle and expands the one behind it allowing it to travel faster than light. Sub-light-speed concepts can be divided in two categories, rocket-derived designs and non. Rocket-derived designs are based on the concept of generating thrust by accelerating mass expelled through a nozzle, this can be achieved in different ways. Both traditional and novel methods are proposed, some of these are for example chemical, nuclear or anti-matter rockets. These however all follow the Tsiolkovsky rocket equation, which limits the achievable change in velocity achievable by any vehicle that carries it's own reaction mass. By eliminating this carried mass this limitation is also removed, so non-rocket-derived design are the preferred choice for this mission. This means that the energy which would otherwise be obtained by the on-board propellant must be transferred to the vehicle remotely. This concept is known as Beam-powered propulsion, and it typically involves electromagnetic waves, such as Laser, to transfer energy. The purpose of this thesis is therefore to study Laser-driven light sails as a method of propulsion for an interstellar journey to Alpha Centauri, verifying it's feasibility in the near future. It will be necessary to derive the physical and structural characteristics that the probe and the laser launch system will have to meet. An overview of the different methods of laser propulsion will be discussed, specifically analysing Laser-driven light sails. Of the latter, two models of motion will be derived and compared, one classical and one that takes into account the relativistic phenomena of which the necessary consideration will be discussed. The material and structural characteristics of the probe proposed and analysed so far will be considered. Finally, other obstacles to overcome during the journey will be evaluated and possible solutions mentioned.

2 Means of Laser Propulsion

Laser propulsion is a type of beam-powered propulsion where the energy source, called Laser Launch System (LLS), is remotely placed in respect of the vehicle and the transfer of power to the vehicle is done through electromagnetic waves (EM). There currently are three main concepts of beamed laser propulsion: Laser Electric Propulsion, Laser Thermal Propulsion and Laser Sails.

2.1 Laser Electric Propulsion

Laser Electric Propulsion (LEP) is a type of laser propulsion where the incoming EM beam is converted to direct current (DC) through a photovoltaic array. This electric power will then be stored on on-board batteries and used in power-electric thrusters such as an ion thruster or plasma propulsion engine. Storing power on-board for a later use is a big advantage over the other propulsion systems here considered. This is a relatively new idea which however is based on an older and already proven concept, that is Solar Electric Propulsion (SEP).

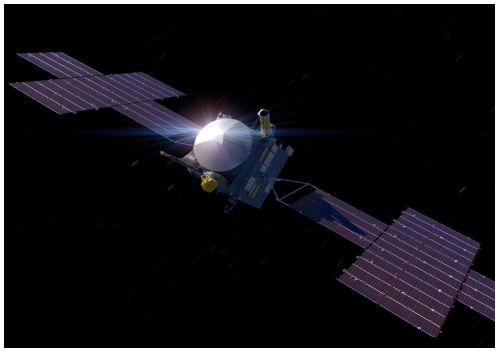

Figure 2:
Illustration of Psyche spacecraft.[2]

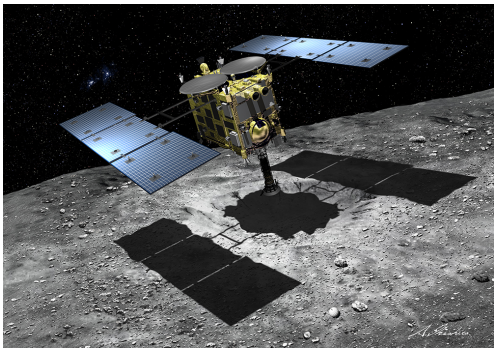

Figure 3:
Illustration of Hayabusa2.[3]

SEP spacecrafts where first conceived in 1966[1] and have since then been tested and used near and far from Earth for decades, for instance on the Hayabusa 1[2] and Hayabusa 2[3] missions launched by the Japan Aerospace Exploration Agency JAXA in 2003 and 2014 respectively and will be used on NASA‘s planned orbiter mission Psyche[4] which is scheduled to launch in 2023. LEP differs from SEP by the use of laser monochromatic light instead of natural astrophysics sources. Laser unlike sunlight have a narrow frequency spectrum and are shown to be able to achieve conversion efficiencies of 55%[5] instead of the 42.8%[6] of Solar light photovoltaics. LEP have already been tested successfully with a 12 hour flight of a laser powered quad-copter called the Pelican by LaserMotive in 2010[7].

[3]Credit: NASA/JPL-Caltech/ASU, Peter Rubin
[3]Credit: Akihiro Ikeshita

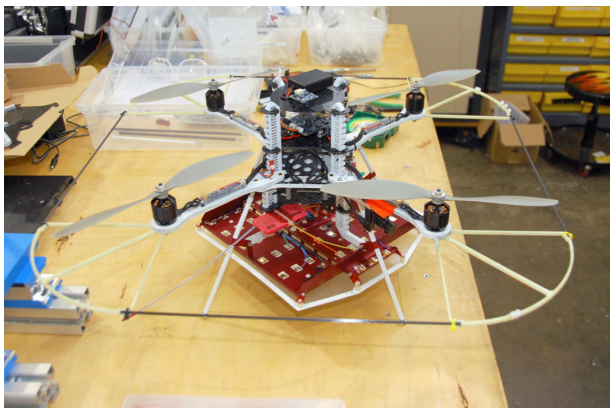

Figure 4: The Pelican quad-copter.[4]

2.2 Laser Thermal Propulsion

Laser Thermal Propulsion (LTP) on the other hand closely resembles solar thermal or nuclear propulsion where, to generate momentum, power is directly transformed into the enthalpy of a working fluid then expanded through a nozzle. In this case the power is obtained through a laser beam separating the power source and its accompanying weight from the vehicle. LTP can be a much less complex system than LEP thanks to the lack of on-board batteries and simpler thruster designs. Laser Thermal Propulsion was firstly conceived by Arthur Kantrowitz [8] in 1971.

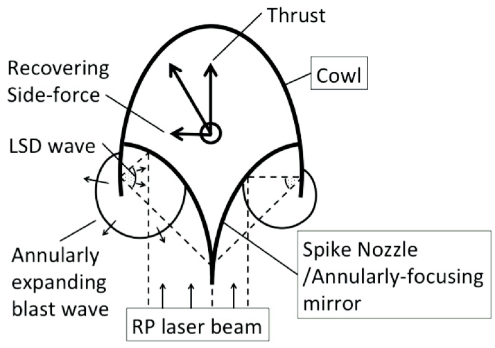

Figure 5:
Myrabo's Lightcraft conceptual drawing.[5]

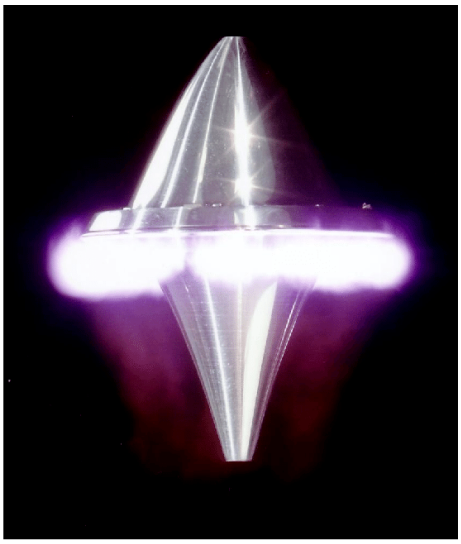

Figure 6: Lighcraft prototype being propelled by laser.[5]

Laser propulsion systems can be divided in two categories: Continuous Wave (CW) and Repetitive Pulse (RP) lasers. RP lasers divide the optical power in pulses of fixed duration at a certain

[4]Credit: Thomas Nugent[7]
[5]Credit: Koichi Mori[9]

repetition rate, these can produce more power in short bursts than CW ones which makes them ideal for Laser Ablative Propulsion (LAP). LAP works by focusing an intense laser pulse (RP in most cases) on a condensed matter surface (gaseous or solid) where a laser-supported detonation produces bursts of either vapor or plasma which, like chemical rockets, produce thrust by the resulting reaction force on the surface. This concept was first envisioned by Kantrowitz [10] in 1972, and was subsequently confirmed experimentally by Myrabo and by Krier. Myrabo's prototype Lighcraft[11] was first tested in 1997 and then in 2000 succeeded in independent vehicle flight guided only by the laser beam with a world record of flight altitude of 71 meters. Myrabo was the first developer of the "beam-riding" concept. Beam-riding happens when the vehicle have to keep its trajectory along the propulsion laser beam, and if the position of the vehicle is deviated then the generated recovery side force will push the vehicle back into the correct trajectory. A similar propulsion method is Pulsed Plasma Propulsion (PPP) where, like LAP, a laser pulse collides on a condensed matter surface which in this case is surrounded by gas, generating heat. The generated heat breaks down the surrounding gas into a plasma which strongly absorbs the incoming pulses generating expanding shock waves called Laser sustained detonation waves or LSD waves. Continuous Wave Lasers output is nominally constant over an interval time, keeping key beam parameters like emitted power, intensity, etc. constant throughout the beam's duration. CW laser propulsion has been studied for laser-sustained plasma (LSP) engines[12] where a lens focuses the incoming laser beam to ignite a plasma which, very similarly to Pulsed plasma propulsion, is then used to heat gaseous propellant in the combustion chamber of a more conventional thruster before being expelled by a rocket nozzle generating thrust.

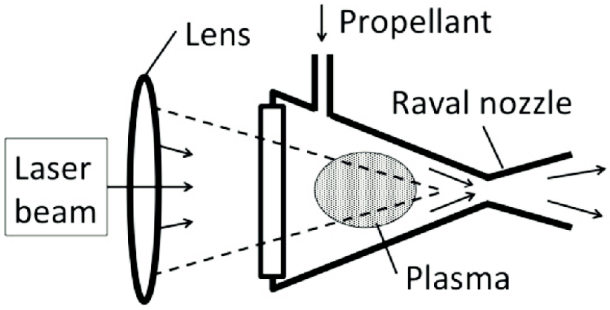

Figure 7: LSP conceptual schematic.[5]

A different kind of LTP is the Heat Exchanger (HX) rocket proposed by Jordin Kare[13] in 1991. In this concept an external laser beams heats a solid heat exchanger, which in turn heats a liquid propellant, converting the laser power to propellant enthalpy turning the on-board propellant into a hot gas that is exhausted through a conventional rocket nozzle. This is a similar concept to PPP and LSP but with the benefit of not needing a precise on-board laser alignment optic system like the other designs.

[5]Credit: Koichi Mori[9]

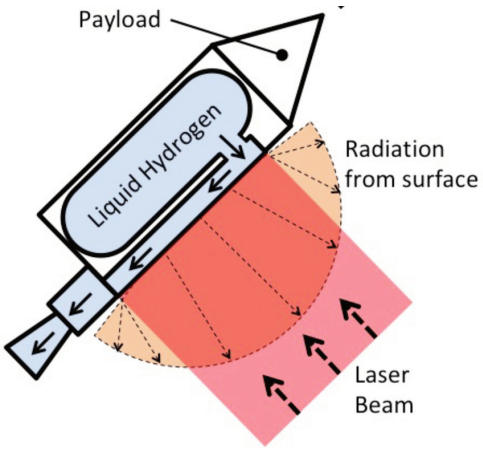

Figure 8: HX rocket conceptual schematic.[5]

Continuous Wave laser propulsion is more complex and generally produce heavier structures than Repetitive Pulse laser propulsion as for the propellant heating is done through an isobaric process so a propellant pump is necessary for an additional compression processes. Similar ideas were conceived using Microwaves instead of Lasers.

2.3 Laser Sails

All of the above concepts necessitate of different kinds of on-board propellant whether it‘s solid or gaseous. This extra mass requires the vehicle structure to be more complex and heavier to account for the reaction mass storage, also this storage structure will remain even after propellant is expelled during the journey. A laser propulsion system that does away with this problem is the laser-sail, first proposed by Georgii Marx[14] in 1966, this system exploits Radiation Pressure Acceleration (RPA) with the benefits that come with using a high power laser source instead of a natural astronomical light source like the ones used by solar-sails.

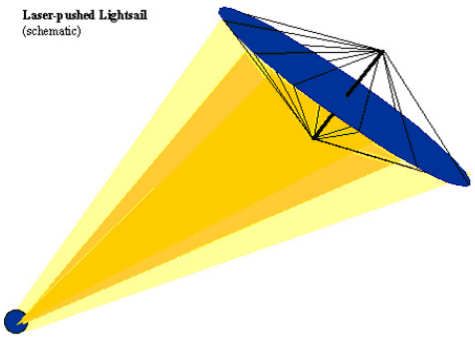

Figure 9: Laser-Sail conceptual image.[6]

[5]Credit: Koichi Mori[9]
[6]Credit: Geoffrey A. Landis

This concept usually involves the use of a powerful laser beam impacting a thin highly reflective film, which is preferred to conventional heavier mirrors. The decoupling of the energy source from the vehicle also gives another advantage as many probes could be launched in a relatively short amount of time thanks to the fact that there needs to be only one stationary launch system which can be used multiple times. Radiation Pressure was first envisioned by Kepler in 1619 when he noticed that all comet tails always pointed away from the Sun. This idea was further put by James Clerk Maxwell with his theory of electromagnetic waves, which affirmed that a electromagnetic radiation, such as light, has momentum and thus can exert a pressure on a opaque striking surface. One of the most important advantages of using laser sources, instead of natural light sources, is that Laser light is monochromatic and coherent (that is with a single wavelength). It‘s wavelength can be precisely tuned to achieve greater power transfer efficiency. This is a tremendous benefit when it comes to sail optimization because, as it will be later discussed, a key parameters for Laser-sails is the sail's reflectance which is closely tied to the wavelength of the incident light. After the first conceptualization of the laser-sail this idea wasn't deemed feasible in the near future until the last decades, when thanks to the recent progress in laser technology the interest in this idea has grown in popularity.

2.4 Sail-type designs

Other similar "sail-type" propulsion are also studied, for example a microwave-pushed sail was proposed by Forward in 1985 with the interstellar probe design called "Starwisp"[15]. This probe would function with a mesh of super thin carbon wires spaced apart by the same length as the wavelength of the incoming microwave beam which would result, in the case of superconductivity, e nearly perfectly efficient mirror.

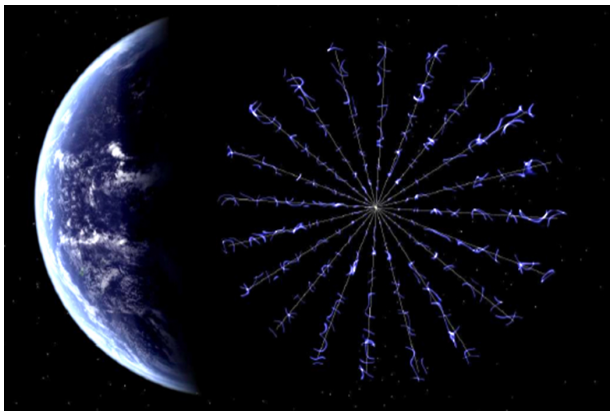

Figure 10: E-Sail conceptual image.[7]

Magnetic Sails[16] work by passing current through a superconductive coil to produces a magnetic field, then if the spacecraft is in movement the interaction between the ions of the

[7]Credit: NASA/MSFC

interstellar medium (ISM) with the magnetosphere of the vehicle leads to a momentum exchange and a thrust on the sail.
Electric sails[17] are a very similar concept to magnetic sails. The sail is made of extended tethers which are charged with a high positive voltage. These charged wires generate an electric field which, by interacting with protons present in the interstellar medium, extracts momentum from these particles generating thrust. The main performance difference between Electric and Magnetic sails is that E-sails have a better efficiency at low speeds, while magnetic sails are superior at higher velocities[18]. A combination of both Magnetic and Electric sails was also proposed, by Perakis[19] for the Dragonfly project competition, which could possibly combine the strengths of both designs. However these two designs do not make use of Laser propulsion so they will not be considered in this study.

2.5 Laser Launch System

A fundamental aspect of beamed power propulsion is the laser power source or the Laser Launch System (LLS). This is the apparatus that must aim and provide a laser beam with the appropriate parameters such as power, beam size and beam direction to the target spacecraft. To realize a LLS with the size and power required for these propulsion types, a cluster that combines a large number of lasers into a coherent phased array is necessary. Directed Energy Phased Array (DEPA) systems are much superior to single aperture systems.

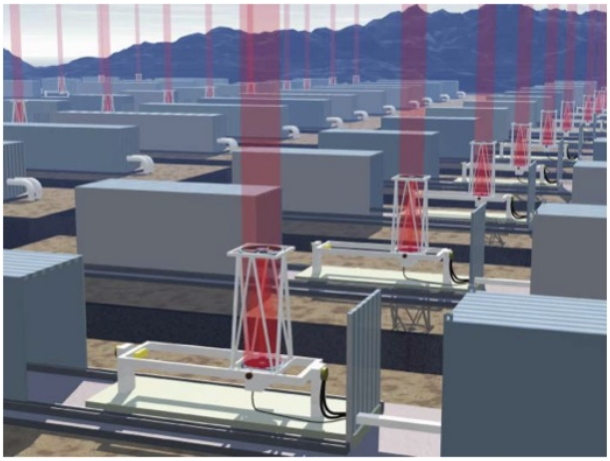

Figure 11: Ground-based Laser array conceptual image.[8]

This is due to the higher scalability of the DEPA infrastructure compared to a monolithic design for both size and power. This makes it much simpler to meet the requirements necessary for the large apertures needed for the long-range targets such as a laser sail. The power needed for laser-sail propulsion can be as high as 100 GW and with a kilometer size aperture. Existing single aperture systems are limited to a meter-class aperture size and maximum of 10kW in

[8]Credit: Jordin Kare

power[20]. To fulfill the Starshot project laser requirements, for example, about 100 million kilowatt-level lasers with a 30 cm aperture would be needed[21]. All of these laser would have to be individually phase-controlled and directionally-guided as, having a coherent phase and alignment for all the single laser beams is imperative to achieve high power transfer efficiency. For a Ground-Based LLS a major challenge to overcome, other than the one posed by standard diffraction, are the effects of atmospheric perturbation like beam wonder, beam expansion and scintillation. These are caused by atmospheric turbulence which cause a local change of the refractive index. Beam wonder refers to the angular deviation of the central axis of the laser beam from the intended direction. Beam expansion, as the name implies, is the variation of additional beam diameter after a long travel inside the atmosphere. Scintillation is caused by the scatter and reflection of light in various directions which will then interfere with itself generating a variation of both power and phase of the signal. A proven way of quantifying the impact of these effects are the Fried parameter r_0 and the isoplanatic angle θ_0. The Fried parameter is defined as the diameter of a circular area over which the root mean square wave front aberration is equal to 1 radian. This is important as, for an aperture D, atmospheric turbulence approximately increases the diameter of the smallest spot by a factor D/r_0 which has to be accounted for, if a diffraction-limited system is desired. The isoplanatic angle θ_0 is the angular difference between the diverted path of light and the desired one. A recent study about this issue[22] found that by placing a large aperture DEPA system at high altitude site a stable diffraction limited spot on a target in space is possible for Fried length $r_0 \geq 10cm$ and Zenith angle ≤ 60 degrees (The angle between the beam direction and the axis perpendicular to the surface). In most proposals the LLS is considered as a Earth-based laser array but in other proposals, like the one formulated by Lubin [23] in 2016 for the Starshot project, an Earth-orbiting set of high power laser is also considered. This laser system is closely based on the Directed Energy System for Targeting of Asteroids and exploRation (DE-STAR) also developed, among others, by Philip Lubin[24].

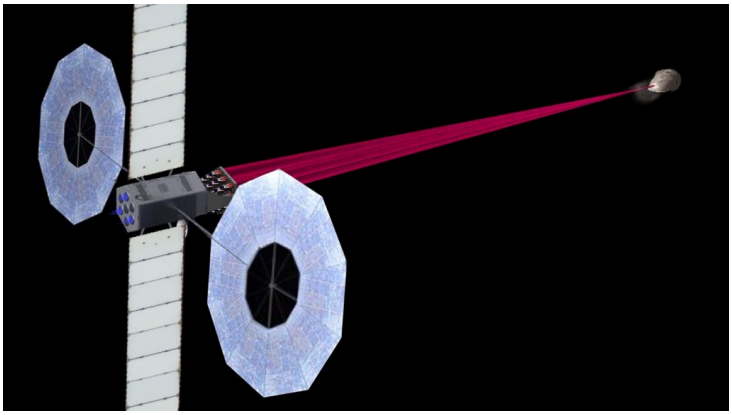

Figure 12: Stand-on DE-STARLITE single launcher based system for planetary defense.[9]

[9]Credit: UCSB Experimental Cosmology Group

This was a project pushed forward by the UCSB Experimental Cosmology group and it's main aim is to use high power Earth-Orbiting Laser arrays to deviate near-Earth objects like meteors and asteroids. These solar powered Laser-phased array systems could achieve a power density of 0.7 GW/Km^2 [24] and would be able to achieve surface spot temperatures of about 3000 K [24], enough to vaporize any known substance. Each DE-STAR is classified by the logarithm of its linear size, so DE-STAR 1 is 10 meters and DE-STAR 2 is 100m. Lubin assessed that a DE-STAR 4 (10 km / 50-70 GW) would be sufficient to propel a meter scale laser sail to around 26% the speed of light with a 10 minutes acceleration phase[23]. An outer-earth LLS have the big advantage of avoiding all atmospheric perturbations and effects that cause a loss in power transfer efficiency to laser propelled spacecraft but with the considerable drawback of being extremely expensive, hard to develop and maintain. This system would also require a powerful propulsion system to maintain its orbit opposing the recoil caused by the emitted beam. A different idea that could mitigate some of the drawbacks was considered by Perakis[19] for the Dragonfly Project competition, a Lunar-Based laser system. This system could mitigate the disadvantages of an Earth-orbiting LLS and combine the advantages of a ground-based LLS, as it would suffer no losses caused by atmospheric perturbations and requires no station keeping.

2.6 Current projects

Initiatives like the Dragonfly Project[25] founded in 2013 from the Initiative for Interstellar Studies aimed to asses the feasibility of laser-sail probes for interstellar spaceflight in the near future. Subsequently in 2014 a design competition for this project was crowdfunded with the design constraints of 100 maximum year travel duration and a 100 Giga-Watts laser beam power to reach the Alpha Centauri system. The participants where six teams formed by students from different Universities around the world. The contest was ultimately won by the team from the Technical University of Munich whose proposal used a lunar-based laser system[19] and also made use of laser-sails for the acceleration phase and a combination of both electric and magnetic sails for deceleration[18]. The University of California, Santa Barbara also funded project Starlight back in 2009 which is also now known as DEEP-IN or Directed EnErgy Propulsion for Interstellar Exploration. This was the foundation from which their team developed their submission for the Project dragonfly competition and has since then evolved into the design for the Breakthrough Starshot project[23]. This project of the Breakthrough Initiatives was founded in 2016 and privately financed by Yuri Milner, Stephen Hawking, and Mark Zuckerberg[26]. Another similar project is the 2069 Alpha Centauri mission concept proposed by NASA which would use a Laser pushed probe to Alpha Centauri 100 years after the famous Apollo 11 moon landing.

3 Laser Propulsion by radiation pressure: theory of the sail

The advantages of having both a lightweight and simpler structure, combined by the high velocities theoretically reachable, makes Laser-sails the most promising proposal to achieve interstellar travel. This spacecraft propulsion method is becoming more and more feasible each year thanks to the progress made in laser systems and sail materials. To study the necessary characteristics of the spacecraft construction and materials, the laser launch system and it's necessities, a mathematical model of motion for the spacecraft is crucial. Further on, a simpler classical motion model and a more comprehensive relativistic motion model will be discussed.

3.1 Classical model derivation

To derive the non relativistic model of motion a similar procedure to the one used by Lubin in [23] will be used. As light carries momentum, The pressure caused by the impact of a radiation on a surface is defined as:

$$\psi_{rad} = \frac{I_b}{c} \tag{1}$$

Where I_b is the Irradiance from the impinging beam on the sail's surface, this is the flux per unit of area of the electromagnetic wave. Pressure radiation force F_{rad} can then be obtained by multiplying the radiation pressure ψ by the sail's surface S_s.

$$F_{rad} = \frac{I_b S_s}{c} \tag{2}$$

On a reflective sail a non zero amount of light will be reflected off of the reflecting surface, this change in direction implies a change in momentum absorbed by the spacecraft.

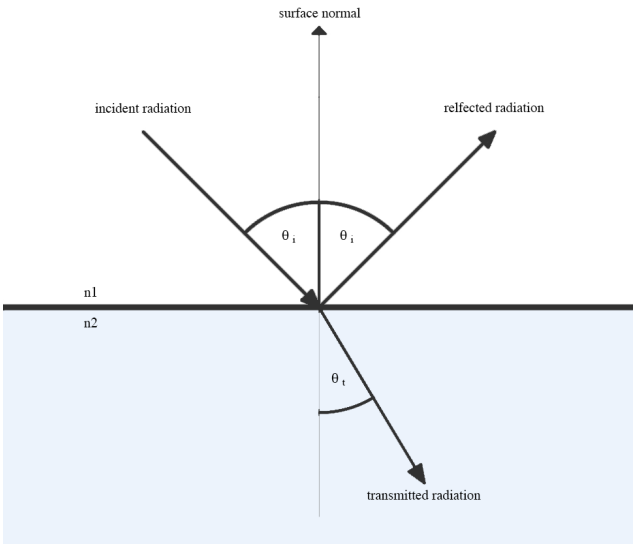

Figure 13: Snell's law of reflection diagram

If the reflector is also partially transmissive and absorbent, the transmitted light will work against the momentum of the spacecraft. These quantities will be accounted for with the Reflectance R, Transmittance T, and Absorbance A coefficients according to Fresnel's refraction equations. And following Snell's relations the impinging power is divided in absorbed, reflected and transmitted power:

$$P_I = (R + A + T)P_I = P_R + P_A + P_T \tag{3}$$

Absorbed power can be, in this case, considered irrelevant to the sail-craft momentum variation, also for this study case the Transmittance coefficient is likewise negligible as it is approximately zero. Only the more simplistic case of a perfectly flat sail surface, which travels perpendicularly to the beam propagation direction, will be here considered. As Irradiance is defined as a power per area, the beam power can be defined such as: $P_I = I_b S_s$.
Radiation pressure force can finally be expressed as:

$$F_{rad} = \frac{S_s I_b}{c} + \frac{S_s I_b R}{c} - \frac{S_s I_b T}{c} = \frac{S_s I_b}{c}(A + 2R) \tag{4}$$

As pressure is a perpendicular force on a surface per unit area, and as force is an acceleration of an object of mass m, the acceleration of the spacecraft of sail's surface S_s and mass $m = m_s + m_p$ (m_s mass of the sail, m_p mass of the payload) can be obtained:

$$a_{rad} = \frac{S_s I_b (A + 2R)}{mc} \tag{5}$$

It is finally noticeable how the acceleration is anti-proportional to the mass of the probe, so a key design factor is to minimize weight. Also it is important to maximize the Reflectance while minimizing the Transmittance and Absorbance of the sail material. Acceleration is constant for a constant power on the sail's surface. It is therefore immediate to derive the velocity from the latter by integrating the acceleration $a(t) = \frac{dv}{dt}$ in the time interval $[0, t]$:

$$v(t) = \int_0^t \frac{S_s I_b (A + 2R)}{mc} dt = \frac{S_s I_b (A + 2R)}{mc} t \tag{6}$$

Using fiducial values taken from the Starshot project the velocity $\beta(t) = v(t)/c$ can be plotted14. With these values the target velocity of $0.2c$ is reached after 1 minute and 31 seconds. The limits of this classic model can also be noticed as after 500 seconds the spacecraft would become faster than the speed of light which is impossible. Another model must then be developed which will have to account for relativistic effects as the spacecraft approaches relativistic speeds.

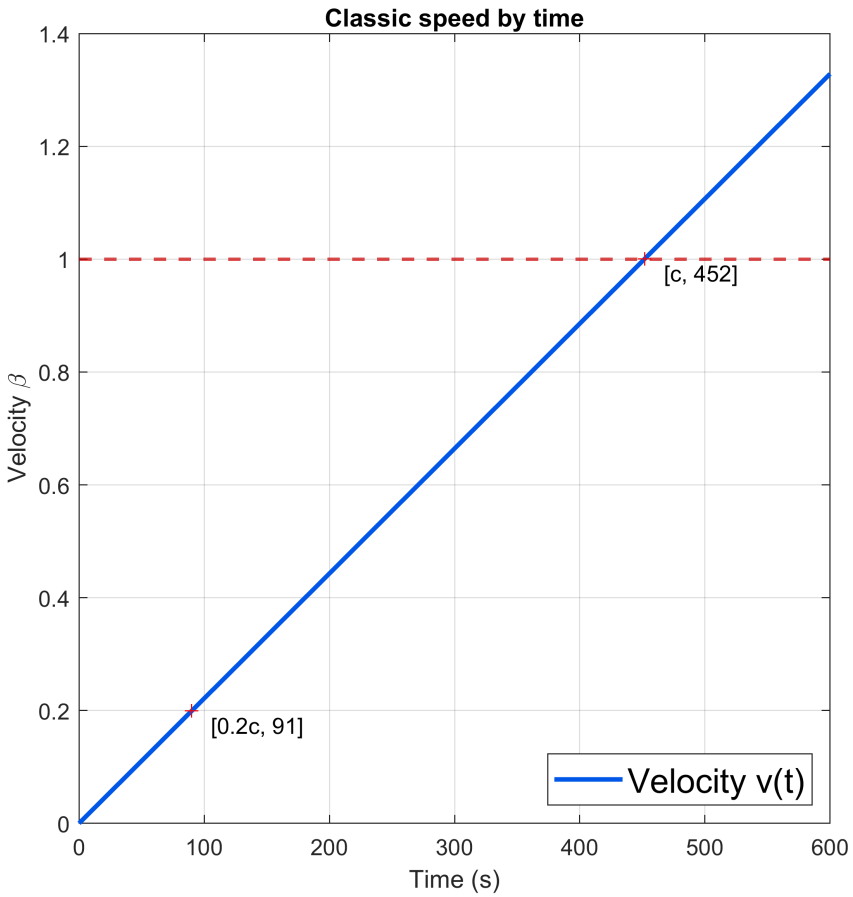

Figure 14: Velocity (v(t)) obtained using the classical model [10]

3.2 Relativistic model derivation

For the relativistic motion model, the same method adopted in [27] will be followed. Given a LLS that can provide a laser beam of constant power P_0, the power that will reach the spacecraft will have to endure a correction. This is due to the change in the photon arrival rate $\Delta\tau$, which is related to the LLS photon departure rate Δt such as: $\Delta\tau = \frac{c}{c-v}\Delta t$. The resulting incident power on the sail is then:

$$P_I(\beta) = P_S(1-\beta) \tag{7}$$

The incident power is no longer constant but a function of $\beta = \frac{v}{c}$ with c being the speed of light and v the spacecraft velocity.

As the spacecraft approaches relativistic speeds ($\beta \longrightarrow 1$), relativistic effects will become non negligible and must be considered. The electromagnetic wave beamed from the LLS will experience a change in it's starting wavelength λ_s due to the relativistic Doppler effect. The incoming beam wave-front moves with speed c, but simultaneously the spacecraft is moving

[10] Parameters: $S_s = 10m^2$, $I_s = 10GW/m^2$, $R = 0.99$, $T \simeq 0$, $m = m_s + m_p = 1g$.

further apart with a velocity v. This, like the standard Doppler effect, causes a change in the frequency of at which wave-fronts arrive at the spacecraft/reflector (r) in the source (s) reference frame:

$$f_r(\beta) = f_s(1-\beta) \tag{8}$$

Due to time dilation however time passes differently in the sail's own reference frame (indicated as *) than the one in the source's reference frame, with their relation being: $t_r^*(\beta) = \frac{t_r}{\gamma}$ where:

$$\gamma = \frac{1}{\sqrt{1-\beta^2}} \tag{9}$$

is the Lorentz factor. As $f = 1/t$ the resulting frequency of the wave impinging on the spacecraft in it's own reference frame is:

$$f_r^*(\beta) = f_r(\beta)\gamma = \sqrt{\frac{1-\beta}{1+\beta}} f_s \tag{10}$$

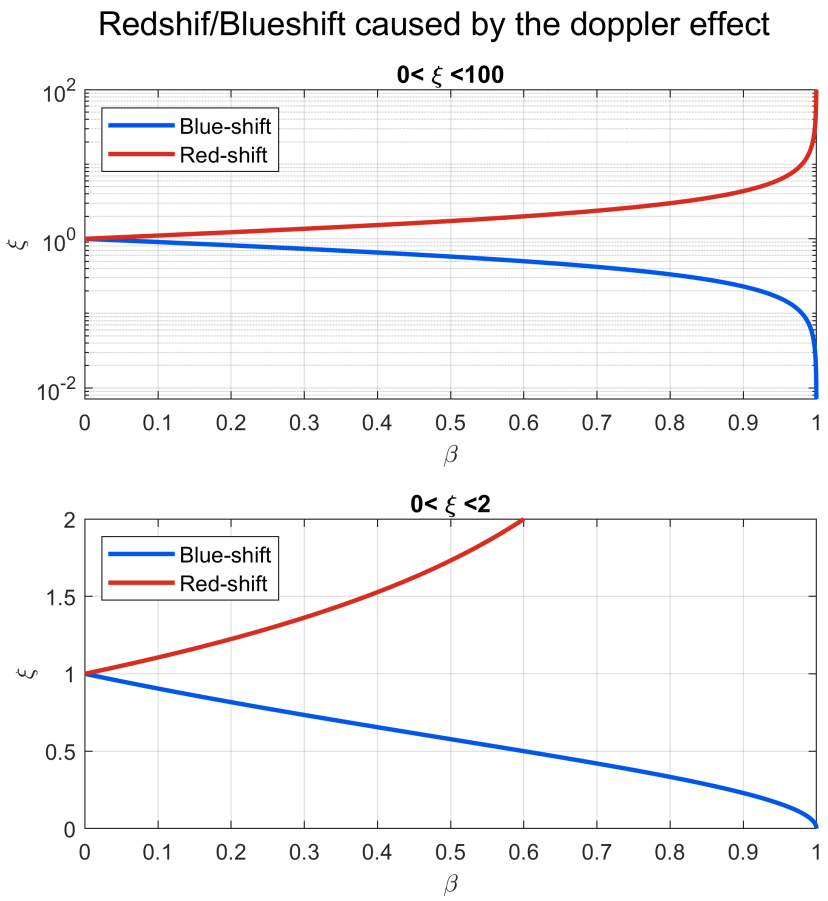

Figure 15: Doppler effect coefficient ξ dependent on β, the upper logarithmic graph shows high values of the coefficient ξ whereas the bottom graph shows small values of ξ.

Converting the wave frequency in it's wavelength results in the relation between the source wavelength, in the source reference frame, and the reflector wavelength in the reflector's reference frame:

$$\lambda_r^*(\beta) = \sqrt{\frac{1+\beta}{1-\beta}}\lambda_s = \xi\lambda_s \tag{11}$$

Where ξ is the Doppler effect multiplication factor. If the source is moving closer to the spacecraft ($v < 0$) the Doppler factor ξ decreases, tending to zero as $\beta \longrightarrow 1$. This is called Blue-shift because, in the visible electromagnetic spectrum, as wavelength decreases it's color shifts to Blue. If the source is moving away from the spacecraft ($v > 0$), ξ increases tending to infinity as $\beta \longrightarrow 1$. This is called Red-shift. By plotting the relation between the relative speed β and the Doppler factor ξ in figure 15it is noticeable how this effects is mild for low relativistic speeds and becomes almost exponential for highly relativistic speeds. For example with $\beta = 0.001$ the observer velocity is $v = 10\,792\,528\,[\frac{Km}{s}]$, this results in an increase of wavelength of only 0.1%. Whereas for $\beta = 0.2$ the wavelength increases by about 22%. The momentum of a single photon is given by:

$$p = \frac{h}{\lambda} = \frac{E}{c} \tag{12}$$

where h is the Planck's constant and E is the photons energy. Power is the amount of energy in a time interval. Power of an electromagnetic wave, counted as the sum of each photon contribution, is also dependent on the observed wavelength. This means that the incident power of an electromagnetic wave undergoes a variation of both it's wavelength component, which is blue-shifted from the Doppler effect (11), and it's time component (7).

$$P_I^*(\beta) = \frac{E}{t} = \frac{ch}{\lambda_r^* t_r^*} = P_S(1-\beta)\sqrt{\frac{1-\beta}{1+\beta}} \tag{13}$$

The beam impinging on the sail surface will then have to obey Snell's laws of reflection, this mean that the incident beam will be partially reflected, partially absorbed and partially transmitted. Fresnel coefficients are dependent on the sail material's refractive index $n(\lambda_r)$, which is strictly dependent on the impinging wave's wavelength and consequently related to the speed β. Reflection and Transmission coefficients can be expressed, with an incident angle normal to the surface, as:

$$R(\lambda_r) = \left(\frac{n(\lambda_r)-1}{n(\lambda_r)+1}\right)^2 \tag{14}$$

$$T(\lambda_r) = \frac{4n(\lambda_r)}{(1+n(\lambda_r))^2} \tag{15}$$

However these will be considered to be constant for this study.

Recalling that the impinging beam is blue-shifted as it approaches the reflector, the same applies for the reflected beam as the observer is moving away from the beam, resulting in a doubly

Doppler shifted wave:

$$P_R^*(\beta, \lambda_s) = P_S(1-\beta)\sqrt{\frac{1-\beta}{1+\beta}}\sqrt{\frac{1-\beta}{1+\beta}}R(\lambda_r) \tag{16}$$

The transmitted beam is instead seeing the observer moving towards it so it will be red-shifted instead :

$$P_T^*(\beta, \lambda_s) = P_S(1-\beta)\sqrt{\frac{1-\beta}{1+\beta}}\sqrt{\frac{1+\beta}{1-\beta}}T(\lambda_r) \tag{17}$$

These can then be simplified:

$$\begin{cases} P_R^*(\beta, \lambda_r) = P_S(1-\beta)R(\lambda_r)\frac{(1-\beta)}{(1+\beta)} \\ P_T^*(\beta, \lambda_r) = P_S(1-\beta)T(\lambda_r) \end{cases} \tag{18}$$

Here it is assumed that as the beam is reflected the same wavelength is kept, David Kipping [28] asserts that this must be false as the reflected photon has reversed momentum and so the reflector must change its momentum for the momentum conservation so kinetic energy must have also increased.

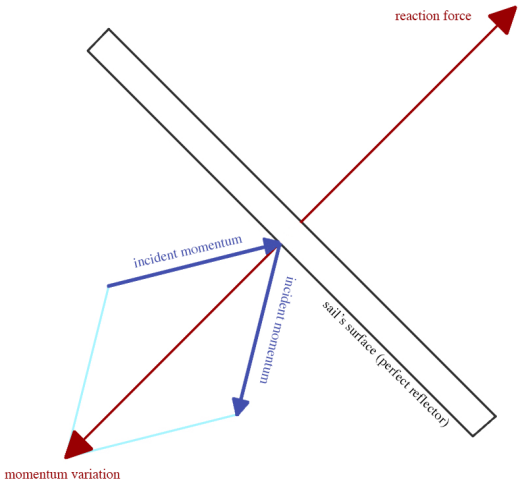

Figure 16: Spacecraft's momentum exchange diagram

To balance the added energy of the system, each photon will have to decrease it's energy by decreasing it's frequency. The absorbed power $P_A = P_I - P_R - P_T$ is the only contribution to the change in internal energy of the vehicle, this can be considered as variation of internal thermal energy.

$$\dot{E} = \dot{m}c^2\gamma + mc^2\gamma^3\dot{\beta}\beta = P_S\frac{(1-\beta)}{(1+\beta)}\left[A(1+\beta) + 2\beta R\right] \tag{19}$$

The variation of momentum of the vehicle is considered as the sum of the contribution of both the impinging power and it's reflected counterpart as, for the elastic collision, the recoil of the reflected photon cause a momentum exchange. The total spacecraft momentum variation also has to account for the transmitted power which contributes negatively in the sum of the contributions. So by taking into consideration the propagation direction and the relation between momentum and energy the following relation can be obtained:

$$c\dot{p} = \dot{m}c^2\gamma\beta + mc^2\gamma^3\dot{\beta} = P_I + P_R - P_T = P_S\frac{(1-\beta)}{(1+\beta)}\left[A(1+\beta) + 2R\right] \tag{20}$$

By combining equations (19) and (20) and simplifying the following system can be written:

$$\begin{cases} mc^2\gamma^3\dot{\beta} = P_S\frac{(1-\beta)}{(1+\beta)}[A+2R] \\ \dot{m}c^2\gamma = P_S\frac{(1-\beta)}{(1+\beta)}A \end{cases} \tag{21}$$

The relation between the time and velocity differentials can be obtained from the first equation of that system and by expressing $d\beta = \frac{\partial\beta}{\partial t}dt$, so to obtain:

$$dt = \frac{mc^2\gamma^3}{P_S[A+2R]}\left(\frac{1+\beta}{1-\beta}\right)d\beta \tag{22}$$

By integrating the instantaneous velocity we can express the traveled distance in the time-frame $[0,t]$ as $X(t) = \int_0^t \beta dt$. And by using the previously derived relation in (22) we can express the travelled distance needed to accelerate the spacecraft from the initial velocity β_i to the final velocity β_f such as:

$$X(\beta_f) = \frac{mc^3}{S_sI_b[A+2R]}\int_{\beta_i}^{\beta_f}\frac{\beta\gamma}{(1-\beta)^2}d\beta \tag{23}$$

And supposing an initial velocity $\beta_i = 0$:

$$X(\beta_f) = \frac{mc^3}{S_sI_b[A+2R]}\left(\frac{(2\beta_f-1)\sqrt{1-\beta_f^2}}{3(\beta_f-1)^2} + \frac{1}{3}\right) \tag{24}$$

The traveled distance $X(\beta_f)$ to reach velocity β_f is obtained. The equation obtained from the relativistic model to one derived from the classical model can be compared, in the limit of $\beta \longrightarrow 0$:

$$X = \frac{mc^3}{S_sI_b[A+2R]}\left(\frac{2}{3}\right) \tag{25}$$

$$x = \frac{2v^2mc}{S_sI_b[A+2R]} \tag{26}$$

By plotting the two equations, for the velocities based on time, the difference between the classic linear and the relativistic solutions is evident.

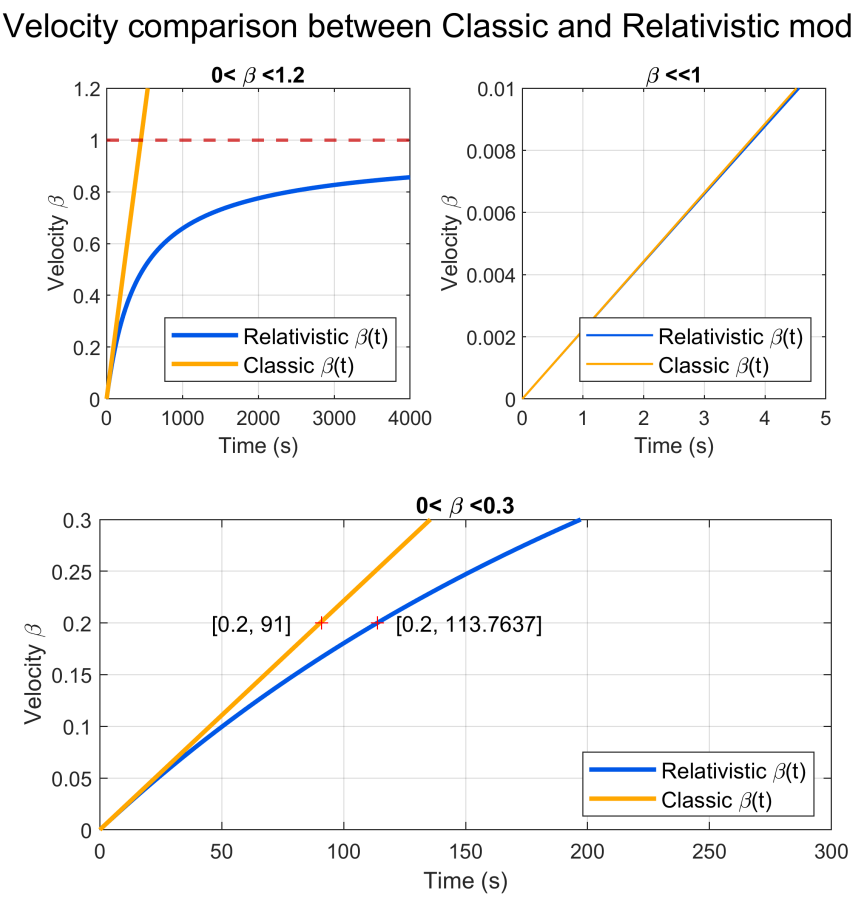

Figure 17: Relativistic vs Classical model velocity (v(t)), for various value ranges of β

With the fiducial parameters from the Starshot project (S_s, I_s, R, A, m) mentioned in Figure 14, the target velocity of $0.2c$ is reached with the relativistic solution after 114 seconds, much longer than the classic solution with 91 seconds. It is also noticeable how the classic model closely approximates the relativistic model as the velocities become smaller fractions of β. But as the velocity approaches β the linear nature of the classic model pushes the velocity value over the limit of β which is impossible. If the relativistic effects were to be ignored, and the acceleration phase time-frame of the probe calculated from the classic model, the prove velocity would be $w\%$ more than the predicted one(with the classic model). This would mean that the probe would most definitely be off the desired route and would miss important encounters with celestial bodies. Being able to reach these velocities would be an incredible achievement. The fastest man-made space probe to this day, the Parker Solar Probe, reached the speed of 393044 km/h or about 109 km/s in February 2020 [29]. To compare this the Parker Solar Probe reached a speed 550 times smaller than the target speed of the probe from this study, which is 0.2c or about 59958 km/s. It would take for the Parker Space Probe around 12 thousand years to reach the Alpha Centauri system, whereas the Laser Propelled probe could potentially only take about 22 years to reach the same destination.

4 Sail's material characteristics

In this section the exigencies for the Laser Launch system and more importantly the sail materials and structure will be discussed. To make an interstellar trip achievable many aspects and complications will have to be endured by the spacecraft, both during it's acceleration phase where the main concern is temperature management and structural rigidity, and it's cruise and possible deceleration phases where the main preoccupation is the interaction between the sail and particles in the interstellar medium. Not less significantly, requirements for the sail and LLS must be feasibly realizable in the near future, as it is a fundamental aspect of making this technology a concrete possibility. During the acceleration phase the sail will be subject to an impinging force, earlier derived, caused by the radiation pressure of the incoming beam, and as explained previously the beam power will be partially reflected, absorbed and transmitted. The main objective is to maximize the percentage of reflected power as this will increase the momentum exchange and indirectly lower the absorbed and transmitted power. It is most important to lower absorbance as the absorbed power will be stored into the sail itself as thermal energy. This is a critical issue as the temperature could rise as much as to damage the spacecraft, as radiative cooling is the sole mechanism for passive thermal management in space. This will be a key constraint in the choice of sail materials, duration time of the acceleration phase and total beam power. First of all, the relation between the laser launch system and the maximum distance for the acceleration phase will have to be determined. Being under the assumption of a diffraction limited laser system, the limiting factor is only the laser spot size, that is the length between the first two minimums of the Airy disk.

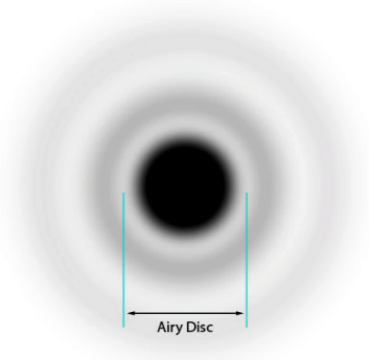

Figure 18: Airy disk conceptual drawing.[11]

So to maintain maximum efficiency in power transfer the laser spot should not exceed the diameter of the sail until the desired velocity β_f is reached, this occurs when the spot size equals the dimension of the sail so when the traveled distance $X(\beta_f)$ equals the diffraction-limited

[11] Credit: Ben Waterman

distance of the LLS:

$$X(\beta_f) \sim Dd_l/2\lambda_s \tag{27}$$

with d_l being the aperture diameter of the LLS [30].
The sail's weight m_s can be expressed as a function of the material area density ρ_s, which also accounts for material thickness, and it's side dimension D such as, for a square sail, $m_s = D^2\rho_s$. Combining these last two equations with equation (24), the relation between the laser array power and size, and the sail dimension and weight requirements can be written as:

$$P_s d_l = 2\lambda_s c^3 \int_0^{\beta_f} \frac{D^2\rho_s + m_p}{D[A+2R]} \frac{\beta\gamma}{(1-\beta)^2} d\beta \tag{28}$$

Taking this equation as function of the sail dimension parameter D, it is minimized for $D^2\rho_s = m_p$, i.e. when the sail mass equal the payload mass. Also it shows that the length of the acceleration distance is proportional to the size of the diffraction-limited laser array. After setting these first constraints, the thermal runaway problem have to be considered. This will have to be avoided by having the sail reach a thermal equilibrium that is non destructive for the structure and components. The time during which the sail will be subject to heating caused by the absorbed power is the acceleration time to reach the target velocity β_f and can be obtained by integrating equation 22 in the optimal mass regime:

$$t = \frac{2\rho_s c^2}{I_b} \left[\int_0^{\beta_f} \frac{\gamma}{(1-\beta^2)[A+2R]} \, d\beta \right] \tag{29}$$

This equation shows that this time duration is only dependent on the beam‘s irradiance while it is independent on the sail‘s surface area dimensions. It is in fact a product of two terms, the characteristic time of the system $t_c = \frac{2\rho_s c^2}{I_b}$ and a term which accounts for the relativistic efficiency of the sail which depends on the optical properties of the light-sail. This last term reaches its minimum of 0.1261 for a perfectly reflective sail with $R = 1$ and $A = 0$. Thermal balance will be achieved when the absorbed power will equal the radiated power, which as the sail is a purely passive device will be modeled as blackbody radiation:

$$P^*_{rad}(T) = D^2 \int_\lambda \epsilon_\lambda(T^*, \lambda) I_{\lambda b}(T^*, \lambda) \, d\lambda \tag{30}$$

Where $\epsilon_\lambda(T)$ is the hemispherical-spectral emissivity(accounting for both surfaces), and $I_{\lambda b}(T)$ is the blackbody spectral intensity. Both these powers are functions of the wavelength λ of the striking electromagnetic beam in the sail's reference frame, which is Doppler shifted throughout the acceleration phase. By considering a laser beam with a source wavelength $\lambda_s = 1064nm$, the wavelength band that will have to be considered, for a target speed of $\beta_f = 0.2c$, is $\lambda_f = 1.22\lambda_s$ or $[1064nm, 1303nm]$. As the wavelength is no longer constant, the same applies to the sail's

absorbency coefficient and consequently the absorbed power:

$$P_A^*(\beta) = P_I^*(\beta)A(\beta) \tag{31}$$

The resulting net power of the sail is then obtained as the difference of the absorbed and radiated power from the previous equations. The temperature change in the sail is a direct result of this stored energy. The time-dependent temperature evolution can now be written as:

$$\frac{\partial T^*}{\partial t^*} = \frac{P_A^* - P_{rad}^*}{C_{sail}} \tag{32}$$

where $C_{sail} = mc_s = 2S_s\rho_s c_s$ is the heat capacity of the sail with c_s being the specific heat capacity. Equation 32 is linearly dependent on the sail‘s surface area through the net power $P_A^* - P_{rad}^*$, simultaneously the heat capacitance also linearly scales with the sail‘s area. This results in the thermal balance of the system being independent on the sail‘s area S_s. Both the thermal balance of the system and acceleration are finally only dependent on the irradiance of the incoming beam I_b and the optical properties of the sail's material.
To derive the final temperature T_0 which the sail will reach at the end of it‘s acceleration phase the thermal equilibrium condition on equations (30) and (31) must be imposed so that the radiated power equals the absorbed power. And by assuming the optimal mass regime the following is obtained:

$$P_I^*(\beta)A(\beta, T_0) = \frac{m_p}{\rho_s}\int_\lambda \epsilon_\lambda(T_0, \lambda)I_{\lambda b}(T_0, \lambda)\, d\lambda \tag{33}$$

This equation can be solved for different values of the ratio m_p/ρ_s and P_s for each material and configuration to provide the equilibrium temperature T_0 dependent on the velocity β. It is also important to mention that the starting temperature of the sail does not affect the thermal evolution of the structure, meaning that the final equilibrium temperature is independent of the starting temperature condition.

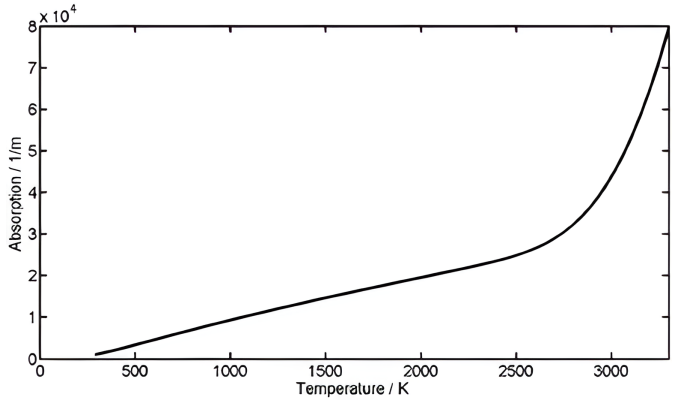

Figure 19: S_iC Absorption dependence on temperature.[12]

[11]Credit: B. Adelmann, Ralf Hellmann[31]

The change in temperature also raise the issue of the change in the sail's material absorption properties. For example in [32] is shown that the absorption coefficient in materials such as silicon has a dramatic increase as temperature increases, taking silicon as an example as it has substantial emissivity in the mid-infrared and low absorption in the near-infrared. The chosen materials to form the sail must have extremely low absorbance ($A < 10^{-5}$) in the near-infrared (IR) even at elevated temperatures to avoid thermal runaway. Simultaneously to allow efficient radiation of thermal energy and maintain equilibrium temperatures below failure levels, high emissivity at wavelengths outside the beam's band is required. By Kirchhoff's law of thermal radiation, high emissivity also implies high out-of-band absorptivity [33]. This places strong constraints in the choice of materials. Commonly used materials for space use such as gold and silver are excellent reflectors in the proposed wavelength range, they however have high enough absorbance to make them unsuitable for this use. Also as previously mentioned, there is a imperative requirement for ultra-low mass structure, which equals to the chosen material having to have very low mass density as well. Following the requirements set by the Starshot project of a sail with surface area of $\sim 10m^2$ and mass of $\sim 1g$, an estimate for the mass density requirement can be made to be about $\rho_s \sim 0.1gm^{-2}$. This means any commonly used mirror material with glass substrate or even materials used on solar sails are unfit for these requirements, and only ultra-thin-film form material will be considered.

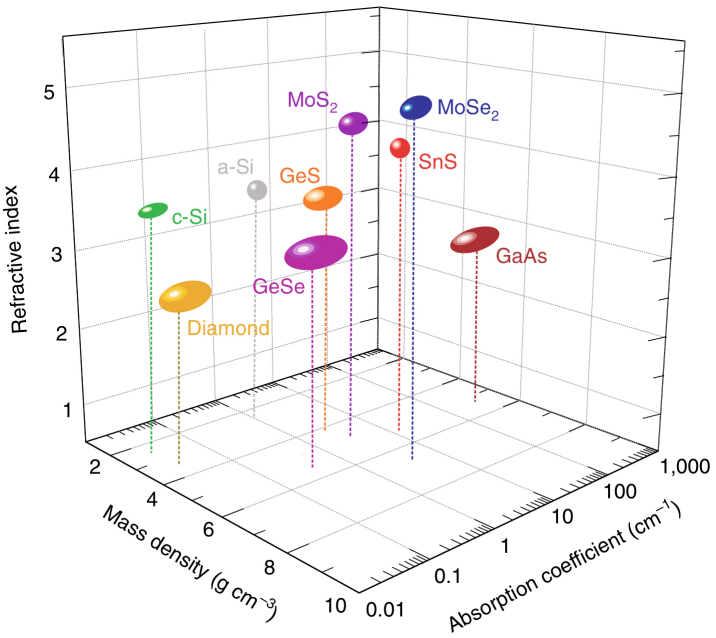

Figure 20: Absorption coefficient, Refractive index and mass density comparison of commonly used materials.[13]

Some examples of material types and structure composition that are currently studied for this application include: two dimensional photonic crystal slabs [34], metasurfaces where arrays of

[12]Credit: Harry Atwater[33]

resonant elements can be jointly exited to modify their reflection profile [35], multilayer stacks of materials with alternating high and low refractive index [27]. A good material candidate with typically high refractive index below the band edge transition energy with low absorbance are semiconductors. In [33] $c-Si$ and MoS_2 where considered as candidate materials having low absorption low mass density and high refractive index. In [30] is shown that thin-film multilayer materials are a preferred choice due to their ability to achieve significant optical contrast for a very low mass. The materials considered and optimised in that study were $Si-SiO_2$. In a more in depth study [27] Si, MgF_2, SiC, SiO_2, Al_2O_3, and TiO_2 were considered in various stack combinations from single up to seven layers. As expected by only considering the acceleration time, the best performing material is a single layer of Si thanks to it's lower mass density and high refractive index. Also Si based structure show greater performance than TiO_2 based ones. Material couples with high optical contrast result in thinner layers, with smaller areal density, and higher propulsion efficiency. This is because structures having lower areal density imply sails of larger size as this is determined by the ratio m_p/ρ_s, for a given payload mass m_p. Considering the thermal evolution of these material the $1064nm$ laser wavelength falls within the absorption gap of Si, this leads to thermal instability of this material even for low irradiance values, so Si based structures will be excluded from further investigations. A suggested solution for Si could be to shift the beam's wavelength range to, for example, $\lambda_s \sim 1.3\mu m$ which would result in a considerable decrease in maximum absorption and increase in light-sail performance. On the contrary TiO_2 based structures show remarkable thermal stability[27] and are able to withstand irradiance values up to $I_b = 100\,GWm^{-2}$. Furthermore considering multilayer compositions instead of single layer, they offer advantages in thermal management, as the maximum critical temperature rises the more layers are added, at the cost of lower acceleration performance. A good compromise of both temperature and acceleration performance are given by 3-layer structures[27]. It is worth noting that the performance of these materials is highly sensitive to the quality of the material as any impurities or defects will impact the level of absorption, so high quality manufacturing processes are a necessity to achieve better material performance. Also while studying the performance of these materials it is significant to mention the importance of precise measurements of the refractive index. In this study case, where it is important to consider that a part of an electric radiation is absorbed into the material, the use of the complex refractive index is required. This can be defined as:

$$\underline{n} = n - ik \tag{34}$$

Where n is the real part of the refractive index, which indicates the phase velocity, and k is the imaginary part also known as the extinction or absorption coefficient which accounts for the amount of attenuation that the wave suffers when passing through a medium. The values for the real part of the refractive index for the aforementioned materials in thin-film form is

widely available in literature, whereas the extinction coefficient is most often not present. As discussed in [33] there is an urgent need to better understand the absorptivity and emissivity of candidate materials for the light-sail as many existing measurements of material absorption focus on the band edge spectral region, or lack the sensitivity to characterize absorption at the ultra low levels required for the light-sail project. This is a key requirements as some of the candidate materials are suitable for this project only for certain k values, so a correct measurement of these is mandatory. In [33] some techniques for ultra-sensitive measurements of the optical properties of these material are proposed. Also new low-weight, low-index materials like aerogels are suggested to be used in this application but further studies are needed as very limited optical data is available on these in a thin-film form. Another area where additional research is necessary is the mechanical stability of these thin-films materials when subject to a high temperature gradient and their ability to withstand the mechanical stresses that challenge the strength of these structures during the acceleration phase. Regarding the first of these two issues, in [27], it is for example suggested that a combination of SiO_2/TiO_2 could withstand this danger. This is because $Si0_2$ show a compressive stress, whereas $Ti0_2$ show a tensile stress when subject to a temperature gradient so they compensate each other when deposited in a multilayer form. Calculations from that study exhibit that a tri-layer SiO_2/TiO_2 structure would suffer a compressive stress of $\simeq -153\,MPa$ and a tensile stress of $\simeq +400\,MPa$ when temperature rise to $700\,K$. And as previous tests have shown SiO_2/TiO_2 dielectric coatings remain stable without layer delamination or coating cracking for thermal cycles up to $\simeq 624\,K$ and show a slight performance drop when rising this to $\simeq 694\,K$. These results could be further enhanced by the use of a substrate which would much improve the stiffness of the structure. Considering now the mechanical strength of the sail structure there is a limited amount of information on the mechanical behavior of thin-film materials in these circumstances. The instantaneous pressure ψ exerted by the impinging beam on the sail's surface can be expressed by normalizing the radiation pressure force F_{rad} acting on it such as:

$$\psi = \frac{I_b}{c}\frac{1-\beta}{1+\beta}\left[(1+\beta)A + 2R\right] \tag{35}$$

Some examples taken from [27] put the maximum pressure experienced by the sail, struck by a beam with irradiance $I_b = 100\,GWm^{-2}$, at $308\,Pa$ with a single layer and $620\,Pa$ for a 7-layer construction. As was predictable with the increase of the number of layer comes an increase in endured pressure. Also the increase in pressure is strictly tied to the irradiance value as seen in figure 21 just like the temperature evolution, so it is obvious that the requirement for the beam power must be minimized as much as possible. The controlled use of the relation between the impinging pressure and the absorption coefficient could be used to solve the challenge of maintaining probe attitude-stability during the acceleration phase.

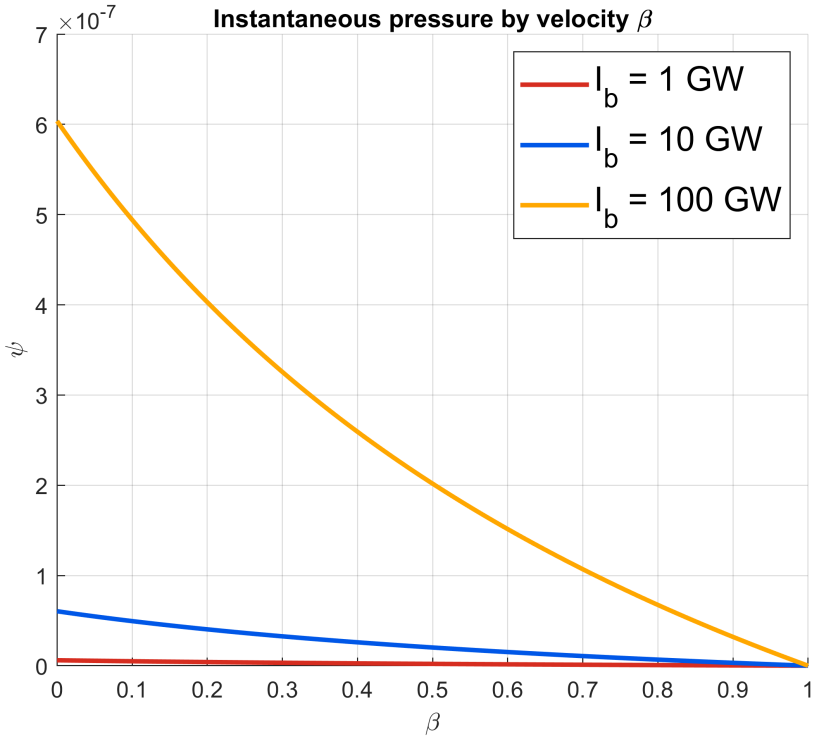

Figure 21: Conceptual graph of instant pressure dependent on the velocity β

Attitude instability can be induced by many factors such as small perturbations in the beam's source or imperfection in the sail's manufacturing. This together with maximizing the probe's acceleration and minimizing heating is going to be a key design consideration to maintain the desired trajectory during this part of the journey. This issue requires to be solved passively through the careful use of structural topology and laser beam profile.

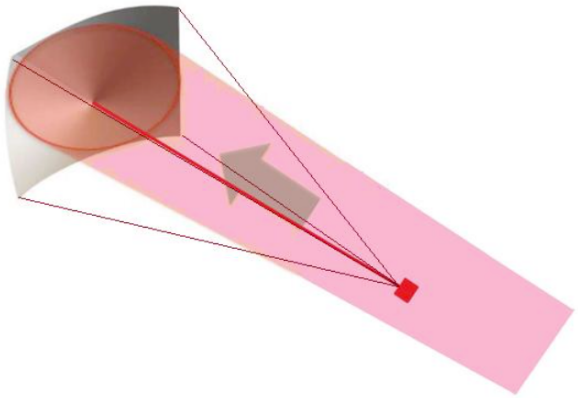

Figure 22: Beam-riding conceptual drawing.[14]

[14]Credit: H. Popova[36]

A possible solution to control the probe's attitude is through the concept of beam riding. Beam riding is the concept of a self-stabilizing vehicle, which works thanks to the topology and structural design of the vehicle that self-corrects misalignment from the beam propagation direction. This is a concept that is already deeply analyzed with the use of a conical-shaped sail riding on a Gaussian beam [36]. Other such solutions like a spherical sail with a multimodal laser beam profile, or the use of a diffraction grating surface, are briefly mentioned in [27]. A more intriguing and novel idea is the use of nanophotonic structures and metasurfaces[35].

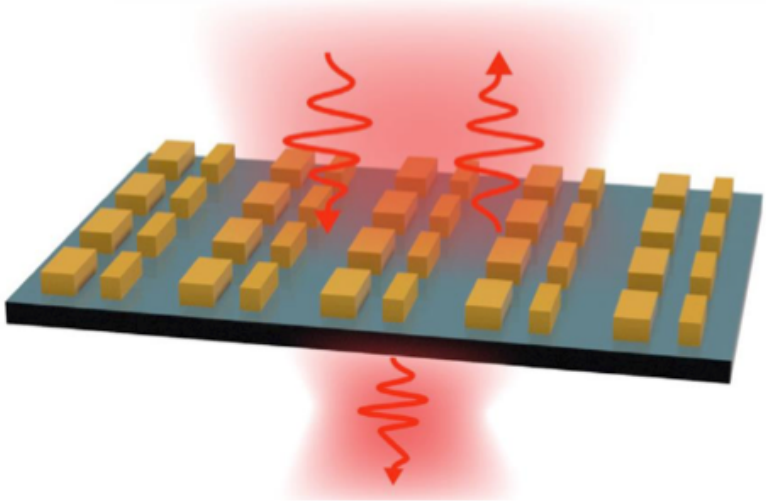

Figure 23: Metasurfaces conceptual drawing.[15]

Metasurfaces are an artificial thin-film material with sub-wavelength thickness. Metasurfaces usually present a periodic array of sub-wavelength-scaled scattering elements in the horizontal dimensions and, thanks to it's thinness compared to the wavelength, these are often used as an interface of discontinuity enforcing an abrupt change in both the phase and amplitude of the impinging radiation. An example of these is the one studied in [38] where a design of a lightweight, low-absorbing, high-reflective, and self-stabilizing curved metasurface made from c-Si nanoparticles was proposed as candidate for this application. A disadvantage that metasurfaces have on multilayer thin-films is the manufacturing process. Coatings like the one used by thin-films are already deposited over large surfaces and with more research and development they will soon be able to reach sub-micrometre levels, whereas metasurfaces are not yet producible in large dimension and the effective scalability of this technology needs further studies. However, trying to produce high quality material with no impurities over large areas can be counterproductive especially if a large volume of this material is desired. A practical solution could be to integrate into the design considerations the use of smaller-scale tiles that can be later joined together to form the final sail structure, some ideas for this solution are mentioned in [33].

[15]Credit: Thomas Pertsch, Yuri Kivshar[37]

5 Coasting and Deceleration phases

After successfully surviving the challenging conditions endured during the acceleration phase, like route misalignment and mechanical/thermal stresses, the probe is now on it's course to the Alpha Centauri system and it's coasting phase begins.

5.1 Coasting phase

During this part of the journey the interaction between the spacecraft and high speed particles present in the space medium are the main concern. As the spacecraft reaches relativistic velocities the danger posed by the impact of a foreign object on the vehicle increases. This is due to the high kinetic energy that can be reached even by minute dust particles at these velocities, these impacts could be powerful enough to damage the probe or alter it's desired route. Kinetic energy is proportional to the velocity squared and can be expressed as following:

$$E_k = m_{particle}\frac{v^2}{2} \tag{36}$$

So even for a particle with a mass as low as 10^{-12} kilograms, the kinetic energy that it carries at a velocity of $0.2c$ is approximately $1800\ Joule$. The journey of this spacecraft through it's coasting phase can be divided in two main portions, interplanetary and interstellar. In the interplanetary travel phase, the sail-craft will have to travel through the solar system, where the main complication is posed by the presence of grains in dust cloud. However the distribution in grain sizes in not properly understood in the specifics yet, this is still a present challenge, but it can also become an opportunity for measurements as the probe exits the solar system. Further research on this topic is still required. Any rough estimates that can be done is to be taken with caution as, considering that the solar system is extremely anisotropic, the amount and type of dust grains present will be very dependent on the exit path chosen. However it can still be useful to get a sense of the danger posed by these impacts. The dust grains contained in the solar system are in size between 100 and $500\ \mu m$. Estimating an average size of $200\,\mu m$ with an approximated density of these particles of $n \sim 10^{-8}\ grains/m^3$ within $50\,AU$ [39]. A grain of this size can be, very broadly, estimated of having a mass of $m_g \sim 10^{-14}\,kg$. A particle with this mass colliding, at a speed of $0.2c$, would have kinetic energy equal to $E_{k_{plan}} \sim 18\,J$. It is necessary to avoid or decrease as much as possible the number of impacts with these particles, one possible solution could be to change the effective surface dimension of the spacecraft orienting it by means of attitude control. Assuming a square shape for the sail's surface $S_s = 10\,m^2$ and rectangular shape for the sail's side surface $T_s = 10^{-6}\,m^2$, with α being the angle between the axis normal to the surface and the direction of motion, the effective area of the spacecraft perpendicular to

the direction of motion can be obtained (figure 25):

$$\sigma_s = S_s cos(\alpha) + T_s sin(\alpha) \tag{37}$$

The total travel distance needed to exit the solar system, perpendicularly to the elliptical plane, is estimated to be around $L = 7\,AU$ or $\sim 10^{12}\,meters$. The total number of collision N between the aforementioned particles and the probe can be calculated like $N = n\sigma_s L$. The results for the previously estimated values are $N_p \sim 10^5$ for the worst case ($\alpha = 0°$) and $N_p \sim 10^{-2}$ for the best case of the planetary phase ($\alpha = 90°$).

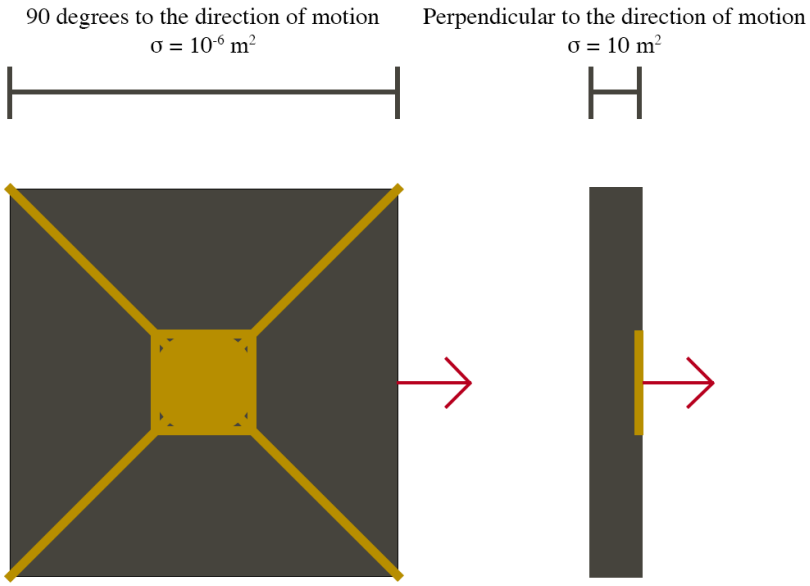

Figure 24: Sail's travel configurations to obtain different cross sections

After the spacecraft escapes the solar system the interstellar section of the journey will begin. The cumulative dust density in the local interstellar medium of the Local Bubble is estimated to be approximately $10^{-6}\,grains/m^3$ for sizes of $500\,nm$ down to $10\,nm$. Assuming a rough average of particle size to be about $100\,nm$ and maximum mass of $m_g \sim 10^{-17}\,kg$, with density of grains of this size inside the Local Bubble estimated to be $n \sim 10^{-9}\,grains/m^3$ [39]. Considering the closest destination for an interstellar trip, the Alpha Centauri system, the travel distance can be approximated to $4.2\,light/years$ or $L \sim 4.2 \times 10^{16}\,m$. Calculating the number of total impacts N_i with the same sail orientation configurations: the worst case collisions ($\alpha = 0°$) result $N_i = 4.2 \times 10^8$ and for the best case ($\alpha = 90°$) $N_i = 4.2 \times 10^1$ impacts. Each of these particle has kinetic energy equal to $E_{k_{int}} \sim 0.018\,J$, thus the total kinetic energy of all of the dust impacts combined can be calculated such as $E_{k(tot)_{int}} = N_i E_{k_{int}}$.

Orientation	**Number of Impacts**	**Total Kinetic Energy**
α	N_i	$E_{k(tot)_{int}}$
Worst case ($\alpha = 0°$)	4.2×10^8	$8 \times 10^6\ J$
Best case ($\alpha = 90°$)	4.2×10^1	$8 \times 10^{-1}\ J$

Making equivalent assessments for the previous interplanetary phase of the trip, the following results are obtained:

Orientation	**Number of Impacts**	**Total Kinetic Energy**
α	N_p	$E_{k(tot)_{plan}}$
Worst case ($\alpha = 0°$)	10^5	$2 \times 10^6\ J$
Best case ($\alpha = 90°$)	10^{-2}	$2 \times 10^{-1}\ J$

These results can be compared with the total kinetic energy of the spacecraft, which with a mass of $m_{tot} = 1\,g$ at a speed of $0.2c$ is equal to $E_{k_{sail}} \sim 2 \times 10^{12}\ J$. By taking a look at the ratio between the kinetic energy of the probe and the one from the impacts $\varkappa = E_{k_{tot}}/E_{k(tot)_{plan}}$ some information can be gathered.

Orientation	**Interplanetary phase Ratio**	**Interstellar phase Ratio**
α	$\varkappa_p$	$\varkappa_i$
Worst case ($\alpha = 0°$)	10^6	$2.5 \times 10^5\ J$
Best case ($\alpha = 90°$)	10^{13}	$2.5 \times 10^{12}\ J$

Keeping in mind that these impacts don't happen all at once and not taking into account the physical damage, the difference in kinetic energy can be considered negligible. This is still true for the worst case scenario as well, as the difference between the spacecraft's kinetic energy and the total one from the particles have several orders of magnitude of difference.

Orientation	**Interplanetary particle Momentum**	**Interstellar particle Momentum**
α	p_p	p_i
Worst case ($\alpha = 0°$)	1.2×10^{-4}	$5 \times 10^2\ J$
Best case ($\alpha = 90°$)	1.2×10^{-11}	$5 \times 10^{-6}\ J$

The same reasoning can be followed to examine the momentum transfer. The total momentum of the dust particles can be obtained as follows $p_{tot} = Np = N\ 2mv$, this is assuming the worst case of a completely elastic collision even if this is highly unlikely. The spacecraft's momentum is equal to $p_{sail} = 1.2 \times 10^5 Nm$. This means that similarly with kinetic energy the momentum exchange can be considered to be negligible, in the worst case there are still several orders of magnitude of difference between the spacecraft's momentum and the one of the dust particles. Even though these impacts with particles through the journey may not mean

an important variation in the desired route and velocity, it does not mean that they cannot cause damage to the spacecraft's structure or electronics. To mitigate the physical damage which may be caused by these impacts on the sail's surface a thin ablative shielding layer could be applied, or the design of the spacecraft could include controlled-damage areas. These could be areas of the sail that would be allowed to be damaged by the particles impacts in a controlled way preventing catastrophic damages while maintaining a predetermined minimum rate of functionality. Another solution could be to minimize the amount of impacts by changing the probe's orientation in regards of the direction of motion by means of attitude control because, as demonstrated above, the number of impacts drastically decreases as the effective surface area decreases. Thus a shielded edge on design could be an enticing solution to this challenge if attitude control is achieved as it would require a much diminished amount of shielding therefore reducing excess weight.

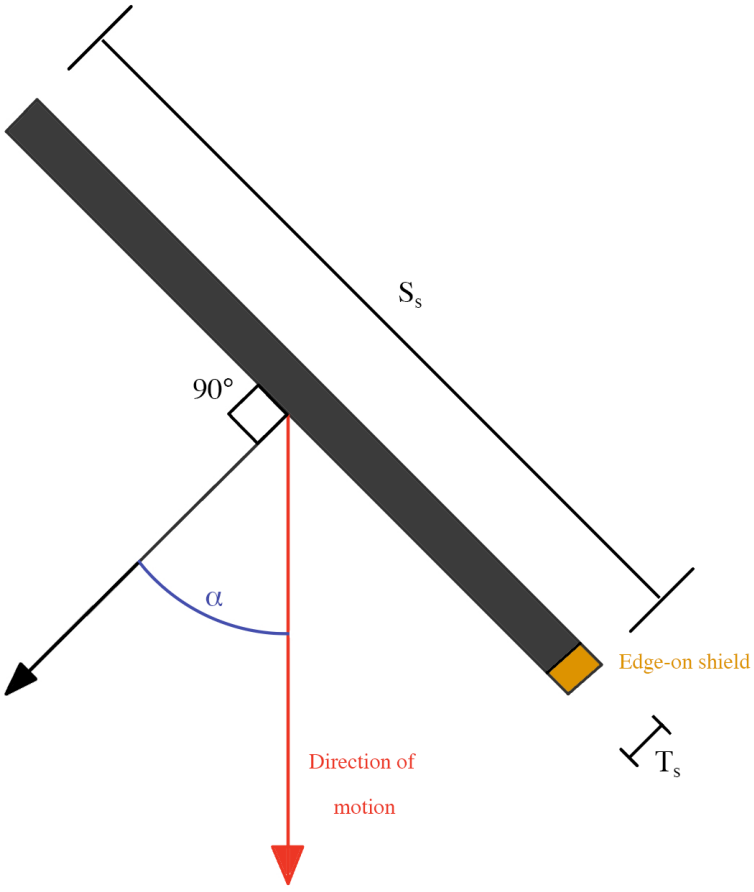

Figure 25: Attitude control schematics

The attitude control system is one that controls the orientation of the spacecraft in respect to an inertial frame of reference. This is essential to have stable and precise trajectory and orientation in space. The predominant proposals for independent attitude control for this application are photon

thrusters or magnetic torquers [23]. Photon thrusters can eject photons to produce thrust, each photon gives a thrust of about $3.3\,nN/W$. There are two main methods for producing photons on a space-probe, the first method uses on-board electrical power to drive laser diodes whereas the second method uses thermal radiation emitted as photons. Magnetic torquer works similarly to magnetic sails, where an electric current passes through looped conductive wires generating a magnetic field. This magnetic field will then interact with the interstellar medium's magnetic field generating controlled thrust force. This sounds promising however the interstellar magnetic field is highly inhomodeneous and anisotropic with a rough average estimate of about $0.1\,nT$. These looped wires could be placed in different positions of the sail and by individually controlling them, the orientation of the probe could be modified. To achieve fully three-dimensional control over the probe would require a three axis torquer, which for a mostly flat spacecraft could be a challenge.

5.2 Deceleration phase

After overcoming the difficulties of the coasting phase the probe is entering the Alpha Centauri system with a velocity of $0.2c$. This enormous speed would make it very complicated to do any imaging of the target system. For example if the spacecraft were to fly by an object of interest at a distance of $r = 1\,AU$, the worst case scenario angular rate would be $\omega = v/r$ which with these parameters would yield $\omega = 4 \times 10^{-4}\,Hz$ or $\sim\ 6 \times 10^{-5}\,rad/s$. This would make difficult to orient the spacecraft and would leave little time before the probe abandons the object of interest, for example with these velocity the probe would traverse $1\,AU$ in about $2500\,s$. Decelerating the probe is perhaps the biggest and most novel challenge of this journey, but one which could massively contribute to the amount of data that could be gathered. One idea could be to use the radiation pressure provided by the star system to slow down the probe. Dissimilarly to the laser launch system used to propel the probe to the target speed, the irradiance of natural radiation emanated from a natural source must obey the inverse square law such as:

$$I_s = \frac{\chi}{4\pi r^2} \tag{38}$$

Where r is the distance from the source and χ is the radiant power. Furthermore when the spacecraft approaches the target, it enters it's gravitational field and is subject to it's gravitational pull. Assuming the sail to be always radially oriented to the center of the star and the star having uniform luminosity, the radiation force operating on the spacecraft can be formulated:

$$F(r) = \frac{S_s L\star}{3\pi c R_\star^2}\left[1 - \left[1 - \left(\frac{R_\star}{r}\right)^2\right]^{3/2}\right] \tag{39}$$

Where $L_\star$ is the star's luminosity $R_\star$ is the stellar radius.

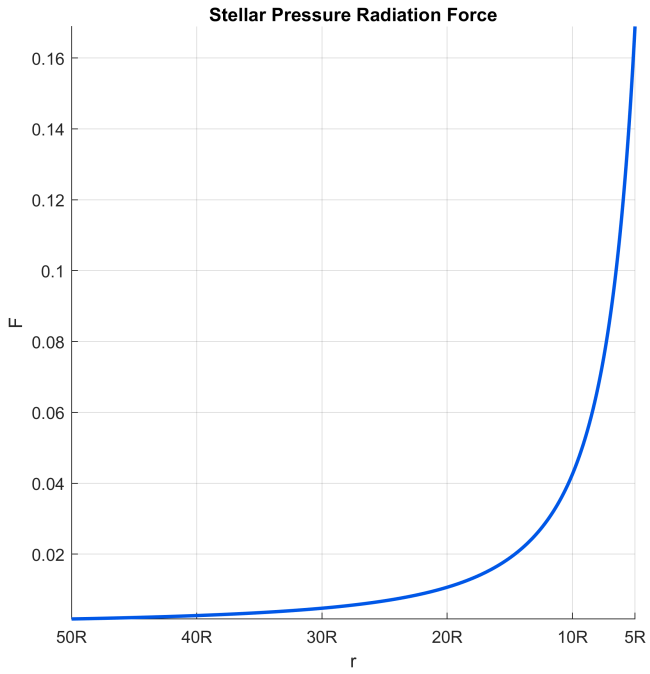

Figure 26: Stellar radiation pressure force calculated with values from [40]

($m = 1\,g$, $S_s = 10\,m^2$, $R_\star = 1.224 R_\odot$ and $L_\star = 1.522 L_\odot$)

A comparable proposal is the one formulated in [40] where a combination of radiation pressure and gravitational assist is studied to slow the spacecraft for a possible orbiting trajectory. In that study the maximum possible reduction in kinetic energy caused by radiation pressure is calculated by integrating equation 39 from the minimum distance that the probe will have from the star r_{min} and infinity the such as:

$$E_{k_{(RP)}} = \int_{r_{min}}^{\infty} F(r)\, dr \tag{40}$$

However the spacecraft is also pulled from the gravitational field of the star, so the variation of potential gravitational energy has to be accounted for:

$$E_{p_{(G)}} = -\frac{GM_\star m}{r_{min}} \tag{41}$$

With G being the gravitational constant, $M_\star$ being the star's mass and m being the spacecraft's mass. To calculate the maximum stopping power of radiation pressure, the condition where the variation of kinetic energy equals the variation of potential energy can be imposed.

$$\Delta v_{max} = \sqrt{\frac{2E_{k_{(RP)}}}{m}} - \sqrt{\frac{2E_{p_{(G)}}}{m}} \tag{42}$$

Δv_{max} is the maximum velocity that the probe must have to be able to fully stop or the maximum speed deficit achievable, for example using the Starshot parameters of a sail with $m = 1\,g$, $S_s = 10\,M^2$ targeting Alpha Centauri A with $r_{min} = 5R_\star$ the result is $\Delta v_{max} = 1.2 \times 10^6\,m/s$ [40]. This deceleration combined with multiple fly-bys on the different stars in the Alpha Centauri system is a promising method of decelerating interstellar light-sails without the use of on-board propellant. Furthermore in [40] it is shown how maximum possible target speed to be able to put the spacecraft in a bound orbit is highly dependent on the sail's density ρ_s, reiterating how innovation in material technology are the main way forward for this project as with a lower density material higher velocities are achievable which directly correlate to smaller mission time. The use of a double-layered reflective sail could be advantageous, where one main layer of the sail's material is optimized for the LLS's beam and the other is instead optimized for the natural radiation emanated from the target star. A more different idea, formulated in [19] for the Dragonfly Project[41], could be to use a combination of both magnetic sails (M-Sails) and electric sails (E-Sails). As mentioned in chapter 2.4 these two methods are able to produce thrust using the interaction of the stationary ions present in the interstellar medium with it's magnetic (or electric) field, which is respectively generated by high current (or voltage) present in superconducting wires when moving at non zero velocity. The use of both systems is particularly beneficial as the two methods complements each other, this is because M-Sails are very efficient at high velocities whereas E-Sails have superior performances at lower speeds. This is more noticeable when observing the force equations of both systems. The force produced by a M-Sail abide by the following equation[42]:

$$F_{M-Sail} = 0.345\pi\sqrt{(m_{proton} n_o \sqrt{\mu} R^2 I)^3}\; v^3 \tag{43}$$

where m_{proton} is the mass of the proton, n_o is the number density of interstellar ions, μ is the free space permeability, R is the radius or the length of the wires, I is the current through the sail and v is the spacecraft's speed. It is apparent from this equation that the force produced scales cubically with the travelling velocity and increases for higher currents and larger dimensions as well, this results in a high efficiency for high speeds. Following the same analysis for the E-Sail, the force produced is dictated by the following equation[43]:

$$F_{E-Sail} = NL\frac{3.09 m_p n_o v^2 r_o}{\sqrt{exp\left(\frac{m_p v^2}{eV_o}\ln\left(\frac{r_o}{r_w}\right)\right) - 1}} \tag{44}$$

Where N is the number of tethers, L is their length, V_o is voltage, e is the electron charge, r_w is the wire radius and r_o is the given by the following equation:

$$r_o = 2\sqrt{\frac{\epsilon_o \kappa_b T_e}{n_o e^2}} \tag{45}$$

With ϵ_o being the electric permittivity of the vacuum, κ_b the Boltzmann's constant and T_e the electron temperature of the interstellar plasma. The relation between the probe's velocity and the produced force is not as clear cut in equation 44 as it was in equation 43. Plotting the force evolution dependent on the velocity for different values of voltage is helpful to understand the nature of this system.

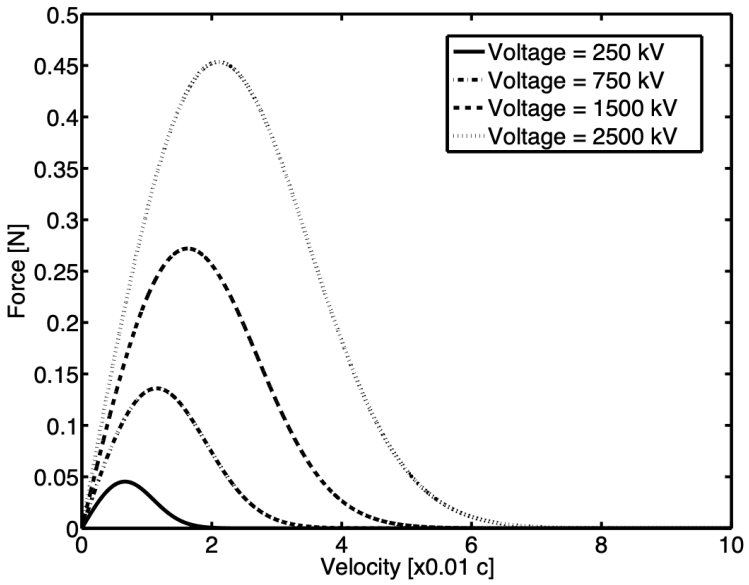

Figure 27: Force on an electric sail as a function of the probe's velocity.[16]

Observing figure 27 it is noticeable how E-Sails are efficient only in a certain working region of the spacecraft's velocity, it is also evident that the working region depends on the voltage value as well as the number and length of the tethers. If the desired working region corresponds to a high velocity then a high voltage and tether requirement follows which also means more mass to carry. This makes E-Sails highly efficient in a small working region, especially for lower velocities given the incremental demands in terms of power and weight for high speeds. The combination of both M-Sails and E-Sails could be an attractive solution for the deceleration problem with some careful measures. Both systems would have to be optimally designed to achieve maximum efficiency in two distinct working region. The high-speed deceleration would be taken care of by the M-Sail system which could be ejected when approaching the E-Sail low-speed working region to decrease total mass of the spacecraft enhancing efficiency. These solutions however still require some type of on-board power supply to function. Furthermore, at the present state, the mass required for these systems greatly exceeds the weight limits for the feasibility of this project. Nevertheless, it cannot be excluded that, with future technological advancements and research, the combination of E-Sails and M-Sails for interstellar deceleration could prove to be a viable solution.

[16]Credit: Nikolaos Perakis[18]

6 Conclusions

As discussed above, the types of propulsion present today day are unsuitable for a journey of this kind, and unlike other exotic methods Laser-driven light sails are based on a technology already existing and tested. The advantages of this propulsion concept are above all: the high speed they can achieve making journeys that would otherwise take thousands of years achievable in a few decades, the lower structural complexity and the ability to launch multiple probes in a relatively small time-frame thanks to the separation of the launch system from the probe itself. Considering that the probe can reach velocities close to that of light it becomes necessary to consider relativistic effects that become significant at these speeds. Therefore two models of motion were derived, a classical and a relativistic model. This was necessary to demonstrate the importance of using the relativistic model because, as discussed above, if they are not considered there are serious differences in the velocity predictions of the probe between the models. This approximation error would cause irremediable errors to the desired route of the trip if they were to be ignored. Considering the construction of the probe, the sail material must withstand the strong forces and high temperatures that will be suffered by the incoming laser beam during the acceleration phase. To maximize performance, the probe must be as lightweight and reflective as possible while trying to minimize it's transmittance and absorbency coefficients as demonstrated by mathematical motion models. Moreover, from equation 28 it has been shown that the case in which the surface area dimension of the sail is optimized, for a certain power of the Laser Launch System's beam, is that in which the mass of the sail and the payload are equal. It has been shown that, given a diffraction-limited system, the maximum distance for the probe to travel during the acceleration phase is closely related to the aperture size of the LLS and it's power. Additionally, the maximum equilibrium temperature reached by the sail was determined based on the rate between characteristics of the material (material density, Absorption and Reflective coefficients) and the power of the incoming laser beam. This also underlines how another fundamental design parameter is the absorption coefficient, which is decisive in the choice of the material according to the selected wavelength range. Another obstacle that must lead to a design consideration was discussed. The presence of space-dust in the interstellar medium poses a threat to the success of the journey, some potential solutions have been mentioned. Also some methods of attitude control to be used during the coasting phase and possible solutions to decrease the probe speed during the deceleration phase were briefly discussed. To date, the necessary technologies to make interstellar travel a reality with Laser-driven light sails are not yet present. There aren't currently phased-laser arrays powerful enough for this application, and no present material can withstand the stresses endured through this journey. However, given the current development rate of laser technologies and materials, it can be assumed that these technologies will become available in the coming years making Laser-driven light sails a true contender to be the technology that will make humans an interstellar species.

References

[1] J. H. MOLITOR, D. BERMAN, R. L. SELIGER, and R. N. OLSON. Design of a solar-electric propulsion system for interplanetary spacecraft. *Journal of Spacecraft and Rockets*, 4(2):176–182, 1967.

[2] Jun'ichiro Kawaguchi, Tono Uesugi, Akira Fujiwara, and Matsuo Hiroki. The muses-c, world's first sample and return mission from near earth asteroid:nereus. *Acta Astronautica*, 39(1):15–23, 1996. Second IAA International Conference on Low-Cost Planetary Missions.

[3] Makoto YOSHIKAWA, Sei ichiro WATANABE, Yuichi TSUDA, Hitoshi KUNINAKA, and Hayabusa2 Project Team. Hayabusa2 - the next asteroid sample return mission of japan. *TRANSACTIONS OF THE JAPAN SOCIETY FOR AERONAUTICAL AND SPACE SCIENCES, AEROSPACE TECHNOLOGY JAPAN*, 12(ists29):29–33, 2014.

[4] Linda T. Elkins-Tanton, Erik Asphaug, James F. Bell, David Bercovici, Bruce G. Bills, Richard P. Binzel, William F. Bottke, Insoo Jun, Simone Marchi, David Y. Oh, Carol A. Polanskey, Benjamin P. Weiss, Daniel Wenkert, and Maria T. Zuber. Journey to a metal world: Concept for a discovery mission to psyche, 2013.

[5] Spectrolab. 044975: 2v, dual-junction gaas power converte. *""*, 2018.

[6] Eli Kintisch. Light-splitting trick squeezes more electricity out of sun's rays. *Science*, 317(5838):583–584, 2007.

[7] Thomas Nugent, Jordin Kare, David Bashford, Carsten Erickson, and Jeff Alexander. 12-hour hover: flight demonstration of a laser-powered quadrocopter. *White Paper*, 2011.

[8] A. KANTROWITZ. Laser population. *Astronatics and Aeronautics*, 10:74, 1971.

[9] Koichi Mori. Beamed launch propulsion. In Alessandro Serpi and Mario Porru, editors, *Propulsion Systems*, chapter 4. IntechOpen, Rijeka, 2019.

[10] Arthur Kantrowitz. Propulsion to orbit by ground-based laser. *Astronaut. Aeronaut.*, 10:74, 1972.

[11] Leik Myrabo, Donald Messitt, and Jr. Franklin Mead. Ground and flight tests of a laser propelled vehicle.

[12] San-Mou Jeng and Dennis Keefer. Theoretical evaluation of laser-sustained plasma thruster performance. *Journal of Propulsion and Power*, 5(5):577–581, 1989.

[13] Jordin T. Kare. Laser-powered heat exchanger rocket for ground-to-orbit launch. *Journal of Propulsion and Power*, 11(3):535–543, 1995.

[14] G Marx. Interstellar vehicle propelled by terrestrial laser beam. *Nature*, 211, 7 1966.

[15] Robert L. Forward. Starwisp - an ultra-light interstellar probe. *Journal of Spacecraft and Rockets*, 22(3):345–350, 1985.

[16] Robert M. Zubrin and Dana G. Andrews. Magnetic sails and interplanetary travel. *Journal of Spacecraft and Rockets*, 28(2):197–203, 1991.

[17] Pekka Janhunen. Electric sail for spacecraft propulsion. *Journal of Propulsion and Power*, 20(4):763–764, 2004.

[18] Nikolaos Perakis and Andreas M. Hein. Combining magnetic and electric sails for interstellar deceleration. *Acta Astronautica*, 128:13–20, 2016.

[19] Nikolaos Perakis, Lukas E. Schrenk, Johannes Gutsmiedl, Artur Koop, and Martin J. Losekamm. Project dragonfly: A feasibility study of interstellar travel using laser-powered light sail propulsion. *Acta Astronautica*, 129:316–324, 2016.

[20] Shawn Redmond, Kevin Creedon, Tso Y. Fan, Antonio Sanchez-Rubio, Charles Yu, and Joseph Donnelly. *Active Coherent Combination Using Hill Climbing-Based Algorithms for Fiber and Semiconductor Amplifiers*, chapter 4, pages 103–136. John Wiley & Sons, Ltd, 2013.

[21] S Pete Worden, Wesley A Green, James Schalkwyk, Kevin Parkin, and Robert Q Fugate. Progress on the starshot laser propulsion system. *Applied Optics*, 60(31):H20–H23, 2021.

[22] Will Hettel, Peter Meinhold, Jonathan Suen, Prashant Srinivasan, Peter Krogen, Allan Wirth, and Philip Lubin. Beam propagation simulation of phased laserarrays with atmospheric perturbations. *Applied Optics*, May 2021.

[23] Philip Lubin. A roadmap to interstellar flight, 2016.

[24] Philip Lubin, Gary B Hughes, Jacob J Bible, Jesse Bublitz, Joshua Arriola, Caio Motta, Jon Suen, Isabella Johansson, Jordan Riley, Nilou Sarvian, et al. Toward directed energy planetary defense. *Optical Engineering*, 53(2):025103, 2014.

[25] Leonard David. Pushing the boundaries: Initiative for interstellar studies, 2014.

[26] F. Jessica. Stephen hawking, mark zuckerberg, yuri milner launch $100m space project called breakthrough starshot. *Nature World News*, april 2016.

[27] Giovanni Santi, Giulio Favaro, Alain Corso, Philip Lubin, Marco Bazzan, Roberto Ragazzoni, Denis Garoli, and Maria Guglielmina Pelizzo. Multilayers for directed energy accelerated lightsails. *Communications Materials*, 3, 04 2022.

[28] David Kipping. Relativistic light sails. *The Astronomical Journal*, 153(6):277, Jun 2017.

[29] Elizabeth Howell. Nasa's superfast parker solar probe just broke it own speed record at the sun. *Space.com*, November 2021.

[30] Ognjen Ilic, Cora Went, and Harry Atwater. Nanophotonic heterostructures for efficient propulsion and radiative cooling of relativistic light sails. *Nano Letters*, 18, 07 2018.

[31] B. Adelmann and Ralf Hellmann. Sic absorption of near-infrared laser radiation at high temperatures. *Applied Physics A*, 122, 06 2016.

[32] H. Rogne, P. J. Timans, and H. Ahmed. Infrared absorption in silicon at elevated temperatures. *Applied Physics Letters*, 69(15):2190–2192, 1996.

[33] Harry Atwater, Artur Davoyan, Ognjen Ilic, Deep Jariwala, Michelle Sherrott, Cora Went, William Whitney, and Joeson Wong. Materials challenges for the starshot lightsail. *Nature Materials*, 17, 05 2018.

[34] John D. Joannopoulos, Steven G. Johnson, Joshua N. Winn, and Robert D. Meade. Photonic crystals: Molding the flow of light - second edition, 2008.

[35] Nanfang Yu and Federico Capasso. Flat optics with designer metasurfaces. *Nature materials*, 13 2:139–50, 2014.

[36] H. Popova, M. Efendiev, and I. Gabitov. On the stability of a space vehicle riding on an intense laser beam, 2016.

[37] Thomas Pertsch and Yuri Kivshar. Nonlinear optics with resonant metasurfaces. *MRS Bulletin*, 45(3):210–220, 2020.

[38] Aso Rahimzadegan, Niels GIESELER, and Carsten Rockstuhl. Self-stabilizing curved metasurfaces as a sail for light-propelled spacecrafts. *Optics Express*, 29, 05 2021.

[39] Andrew R. Poppe. An improved model for interplanetary dust fluxes in the outer solar system. *Icarus*, 264:369–386, 2016.

[40] René Heller and Michael Hippke. Deceleration of high-velocity interstellar photon sails into bound orbits at α centauri. *The Astrophysical Journal*, 835(2):L32, feb 2017.

[41] Tobias Häfner, Manisha Kushwaha, Onur Celik, and Filippo Bellizzi. Project dragonfly: Sail to the stars. *Acta Astronautica*, 154:311–319, 2019.

[42] Freeland II. Mathematics of magsails. *JBIS - Journal of the British Interplanetary Society*, 68:306–323, 01 2015.

[43] Pekka Janhunen and A Sandroos. Simulation study of solar wind push on a charged wire: basis of solar wind electric sail propulsion. *Annales Geophysicae*, 25:755–767, 2007.

List of Figures

1 Light-Sail concept . . . 1
2 Psyche conceptual drawing . . . 3
3 Hayabusa2 conceptual drawing . . . 3
4 The Pelican . . . 4
5 Lightcraft conceptual drawing . . . 4
6 Lightcraft prototype . . . 4
7 LSP conceptual schematic . . . 5
8 HX rocket conceptual schematic . . . 6
9 Laser-Sail conceptual image . . . 6
10 E-Sail conceptual image . . . 7
11 LLS concept image . . . 8
12 DE-STAR concept image . . . 9
13 Snell's law of reflection diagram . . . 11
14 Classical model velocity graph . . . 13
15 Doppler coefficient graphs . . . 14
16 Spacecraft's momentum exchange diagram . . . 16
17 Relativistic vs Classical model velocity (v(t)), for various value ranges of β . . . 18
18 Airy disk conceptual drawing . . . 19
19 Absorption/Temperature graph . . . 21
20 Common material's optical parameters . . . 22
21 Conceptual graph of instant pressure dependent on the velocity β . . . 25
22 Beam-riding conceptual drawing . . . 25
23 Metasurfaces conceptual drawing . . . 26
24 Sail's travel configurations to obtain different cross sections . . . 28
25 Attitude control schematics . . . 30
26 Stellar radiation pressure force calculated with values from [40] . . . 32
27 E-Sail force graph . . . 34

Acknowledgements

I would like to express my sincere gratitude to my professor and supervisor Dr. Maria Guglielmina Pelizzo for her invaluable patience and feedback. I could not have undertaken this work without her generously provided knowledge and expertise. Additionally I want to thank all the other professors and students of the University of Padova who taught and inspired me during the course of these years.

Not a day goes by without reflecting on the sacrifices that my parents made to make sure that I could pursue my studies without any worries, so I want to thank immensely my father Corrado and my mother Paola for their endless love and support. You are my inspiration and role models and your constant teachings have made me what I am today.

I am thankful to my brother who helped me many times along the way and was always there ready to advise and annoy me.

Thanks to all of the uncles, aunties and cousins from whom I could take advice that helped me grow as a person.

A heartfelt thanks to the grandparents who are no longer here but who I continue to carry with me at all times.

I would be remiss in not mentioning my friends and my girlfriend. Their belief in me has kept my spirits and motivation high through good and hard times